Synthesis, Ion Aggregation, Alkyl Bonding Modes, and Dynamics of 14-Electron Metallocenium Ion Pairs [(SBI)MCH$_2$SiMe$_3^+$···X$^-$] (M = Zr, Hf): Inner-Sphere (X = MeB(C$_6$F$_5$)$_3$) versus Outer-Sphere (X = B(C$_6$F$_5$)$_4$) Structures and the Implications for "Continuous" or "Intermittent" Alkene Polymerization Mechanisms

Fuquan Song,[†] Simon J. Lancaster,[†] Roderick D. Cannon,[†] Mark Schormann,[†] Simon M. Humphrey,[‡] Cristiano Zuccaccia,[§] Alceo Macchioni,*[,§] and Manfred Bochmann*[,†]

Wolfson Materials and Catalysis Centre, School of Chemical Sciences and Pharmacy, University of East Anglia, Norwich NR4 7TJ, U.K., University Chemical Laboratory, University of Cambridge, Cambridge CB2 1EW, U.K., and Dipartimento di Chimica, Università di Perugia, 06123 Perugia, Italy

Received September 29, 2004

The new mixed-alkyl metallocene complexes (SBI)M(Me)CH$_2$SiMe$_3$ (M = Zr, Hf) are accessible by the successive treatment of (SBI)MCl$_2$ with Me$_3$SiCH$_2$MgCl and MeMgCl in toluene (SBI = *rac*-Me$_2$Si(1-Ind)$_2$). Reaction with B(C$_6$F$_5$)$_3$ or CPh$_3^+$[B(C$_6$F$_5$)$_4$]$^-$ in toluene or toluene/difluorobenzene affords (SBI)M$^{\delta+}$(CH$_2$SiMe$_3$)(μ-Me)B$^{\delta-}$(C$_6$F$_5$)$_3$ and the ion pairs [(SBI)MCH$_2$SiMe$_3^+$···B(C$_6$F$_5$)$_4^-$], respectively. Both types of compounds are thermally stable in aromatic solvents at ambient temperature. Whereas in the MeB(C$_6$F$_5$)$_3^-$ complexes the alkyl ligand points away from the metal and tight anion coordination forms the familiar inner-sphere ion pair, in the B(C$_6$F$_5$)$_4^-$ salts the alkyl ligand adopts a conformation that enables agostic bonding to a γ-CH$_3$ group. Here, and by implication in M-polymeryl species of similar steric requirements, agostic interactions are preferred over anion coordination, leading to an outer-sphere ion pair structure. This alkyl bonding mode retards the −SiMe$_3$ rotation, which for M = Hf is slow on the NMR time scale at −20 °C (at 300 MHz), while in the zirconium analogue cooling to below −60 °C is required. It was shown that chain swinging involves a 180° rotation of the alkyl ligand about the Zr−C bond. Measurements of diffusion coefficients by pulsed field gradient spin−echo (PGSE) techniques suggest that while (SBI)Zr(CH$_2$SiMe$_3$)(μ-Me)B(C$_6$F$_5$)$_3$ exists in solution as mononuclear zwitterions as expected, [(SBI)ZrCH$_2$SiMe$_3^+$···B(C$_6$F$_5$)$_4^-$] forms ion quadruples ([Zr] ≈ 2 mM), rising to hextuples at higher concentration. The relative positions of cations and anions depend on the ion pair concentration; higher aggregates make it difficult to assign specific anion positions. The rate of ion pair symmetrization ("anion exchange" k_{ex}), as determined by variable-temperature NMR spectroscopy, decreases with decreasing metallocene concentration. For [(SBI)ZrCH$_2$SiMe$_3^+$···B(C$_6$F$_5$)$_4^-$] at 25 °C and [Zr] = 2 mM, $k_{ex} \approx 500 \pm 170$ s^{-1}; this value represents the upper limit of anion mobility expected under catalytic conditions where concentrations are typically 100 times lower. Ion pair symmetrization rates are therefore at least 1 order of magnitude slower than the growth of the number-average molecular weight of polypropene chains (k_p[M] ≈ 10^4 s^{-1} at [M] = 0.59 mol L^{-1}) generated with tetraarylborate-based (SBI)Zr and other high-activity catalysts at identical temperatures. It is suggested that while for slower, inner-sphere ion pair catalysts the rate of 1-alkene consumption is commensurate with k_{ex} ("continuous" chain propagation mechanism), high-activity catalysts may operate by a mechanism where the anion does not bind to the metal center and so does not limit the rate of monomer enchainment. In such a situation, agostic metal−alkyl interactions form the catalyst resting states in preference to anion coordination.

Introduction

Metallocenium cations of group 4 metals paired with very weakly coordinating anions, [L$_2$MR$^+$····X$^-$] (M = Ti, Zr, Hf), are now well recognized as the active species in metallocene-based alkene polymerization catalysts.[1−4]

* To whom correspondence should be addressed. E-mail: m.bochmann@uea.ac.uk.
[†] University of East Anglia.
[‡] University of Cambridge.
[§] Università di Perugia.

(1) Reviews: (a) Bochmann, M. *J. Organomet. Chem.* **2004**, *689*, 3982. (b) Chen, E. Y. X.; Marks, T. J. *Chem. Rev.* **2000**, *100*, 1391. (c) Bochmann, M. *J. Chem. Soc., Dalton Trans.* **1996**, 255. (c) Jordan, R. F. *Adv. Organomet. Chem.* **1991**, *32*, 325.
(2) Brintzinger, H. H.; Fischer, D.; Mülhaupt, R.; Rieger, B.; Waymouth, R. *Angew. Chem., Int. Ed. Engl.* **1995**, *34*, 1143.

10.1021/om049248d CCC: $30.25
Publication on Web 02/12/2005

While aspects such as the stereo- and regioselectivity of 1-alkene polymerizations can be explained by considering the structure of the metallocenium alkyl cation only,[2,4] more detailed mechanistic studies have recently highlighted the importance of the counteranion X during the polymerization process and its role in controlling catalyst activity, stereoselectivity, and polymer molecular weight.[1a,5−8] For example, it could be shown that the anion modulates the energy of the transition state and that anion mobility is related to catalyst activity.[6,9] The observation that under comparable conditions some metallocenes such as (SBI)$ZrCl_2$ (SBI = *rac*-$Me_2Si(1\text{-}Ind)_2$) are substantially more active if activated with $AlBu^i_3/CPh_3^+[B(C_6F_5)_4]^-$ than with methylalumoxane (MAO)[10] has been shown to be largely due to anion-dependent variations in the lifetimes of the catalytic intermediates, rather than due to differences in the concentration of active species.[11] Studies of the polymerization kinetics and of the solution behavior of metallocenium ion pairs have demonstrated that in low-polarity solvents such as toluene there is no free diffusion of ions out of the solvent cage.[11,12]

It has also become apparent that the solution structure of metallocenium ion pairs may be more complex than the simple ion pair formulation suggests. Brintzinger et al. provided evidence that, at least at the concentration employed for these studies and in aromatic solvents, ion pairs join together to form quadruples or higher aggregates.[13] The tendency for such aggregation is of course dependent on the degree of ionic character of the ion pair; compounds that form mononuclear zwitterions in the solid state, such as the methylborates $L_2ZrMe(\mu\text{-}Me)B(C_6F_5)_3$, also exist in solution as mononuclear tight (or inner-sphere) ion pairs.[13a,14] On the other hand, if a donor ligand D is added to give ionic outer-sphere compounds of the type $[LL'ZrMe(D)]^+X^-$, or if the metallocene structure is sufficiently open to form solvent complexes (D = benzene or toluene) as in the case of half-sandwich and constrained-geometry compounds, higher ion aggregates will result, independent of the nature of the anion.[13,14b]

Ion pairs $[L_2MR^+\cdots X^-]$ are fluxional systems that readily undergo site exchange of R and X.[1a,13b,15] Since anion displacement equilibria and site epimerization are integral parts of the polymerization process, these data provide important mechanistic information. Most such studies to-date have been carried out on zirconocene methyl complexes as model systems. However, while the generation of methyl compounds is convenient, a CH_3 ligand is a less than ideal representation of a polymeryl chain since it has a much smaller steric demand, shows no conformational preferences, and is capable of forming methyl-bridged binuclear complexes. We were therefore interested in the fluxionality and aggregation properties of complexes with longer and bulkier alkyl chains as more realistic catalyst models. Here we report the synthesis, solution behavior, and ion pair dynamics of metallocenium ion pairs bearing the trimethylsilylmethyl ligand, $[(SBI)MCH_2SiMe_3^+\cdots X^-]$ (M = Zr, Hf; X = $MeB(C_6F_5)_3$ or $B(C_6F_5)_4$). The structures of these catalysts, their site epimerization rates, and the nature of the metal−anion interaction differ fundamentally between the two types of anion, with implications for the kinetic regime of alkene polymerizations operative in high-activity catalysts. The propene and 1-hexene polymerization kinetics with $[(SBI)ZrCH_2SiMe_3^+\cdots X^-]$ as catalysts have been the subject of a preliminary communication.[16]

Results and Discussion

Synthesis. The reaction of (SBI)$ZrCl_2$ (**1**) (SBI = *rac*-$Me_2Si(1\text{-}Ind)_2$) with 1 equiv of Me_3SiCH_2MgCl in toluene gives cleanly the monoalkyl complex (SBI)$ZrCl(CH_2SiMe_3)$ (**2**). Further reaction with MeMgCl affords the mixed-alkyl complex (SBI)$ZrMe(CH_2SiMe_3)$ (**3**). The latter is conveniently synthesized from **1** in a one-pot reaction by successive additions of Me_3SiCH_2MgCl followed by MeMgCl. Preparation of the hafnium analogue of **2**, (SBI)$HfCl(CH_2SiMe_3)$ (**5**), is less facile, and (SBI)$HfCl_2$ (**4**) must be treated with an excess of Me_3SiCH_2MgCl in toluene at 80 °C overnight to ensure complete conversion. (SBI)$HfMe(CH_2SiMe_3)$ (**6**) can be prepared in a fashion very similar to **3** by methylating **5** with MeMgCl (Scheme 1). Related mixed-alkyl complexes of zirconocenes with nonbridged cyclopentadienyl ligands have recently been reported.[17]

Compounds **2**, **3**, **5**, and **6** are obtained as pale yellow crystalline solids. The ^1H NMR spectra confirm C_1 symmetry. The M-CH_2 hydrogen atoms are diaste-

(3) Bochmann, M.; Jaggar, A. J.; Nicholls, J. C. *Angew. Chem., Int. Ed. Engl.* **1990**, *29*, 780.
(4) (a) Cavallo, L.; Guerra, G.; Vacatello, M.; Corradini, P. *Macromolecules* **1991**, *24*, 1784. (b) Ewen, J. A.; Elder, M. J. *Makromol. Chem., Macromol. Symp.* **1993**, *66*, 179. (c) Canstongay, L. A.; Rappé, A. K. *J. Am. Chem. Soc.* **1992**, *114*, 5832. (d) Hart, J. R.; Rappé, A. K. *J. Am. Chem. Soc.* **1993**, *115*, 6159. (e) Guerra, G.; Cavallo, L.; Moscardi, G.; Vacatello, M.; Corradini, P. *J. Am. Chem. Soc.* **1994**, *116*, 2988. (f) Leclerk, M. K.; Brintzinger, H. H. *J. Am. Chem. Soc.* **1995**, *117*, 1651. (g) van der Leek, Y.; Angermund, K.; Reffke, M.; Kleinschmidt, R.; Goretzki, R.; Fink, G. *Chem. Eur. J.* **1997**, *4*, 585. (h) Busico, V.; Cipullo, R.; Caporaso, L.; Angelini, G.; Segre, A. L. *J. Mol. Catal. A: Chem.* **1998**, *128*, 53.
(5) (a) Yang, X.; Stern, C. L.; Marks, T. J. *Organometallics* **1991**, *10*, 840. (b) Jia, L.; Yang, X.; Stern, C. L.; Marks, T. J. *Organometallics* **1997**, *16*, 842. (c) Chen, Y. X.; Stern, C. L.; Marks, T. J. *J. Am. Chem. Soc.* **1997**, *119*, 2582. (d) Metz, M. V.; Schwartz, D. J.; Stern, C. L.; Nickias, P. N.; Marks, T. J. *Angew. Chem., Int. Ed.* **2000**, *39*, 1312. (e) Sun, Y.; Metz, M. V.; Stern, C. L.; Marks, T. J. *Organometallics* **2000**, *19*, 1625.
(6) Zhou, J.; Lancaster, S. J.; Walker, D. A.; Beck, S.; Thornton-Pett, M.; Bochmann, M. *J. Am. Chem. Soc.* **2001**, *123*, 223.
(7) (a) Siedle, A. R.; Lamanna, W. M.; Newmark, R. A.; Stevens, J.; Richardson, D. E.; Ryan, M. *Makromol. Chem. Macromol. Symp.* **1993**, *66*, 215. (b) Chien, J. C. W.; Song, W.; Rausch, M. D. *J. Polym. Sci. Part A: Polym. Chem.* **1994**, *32*, 2387.
(8) (a) Herfert, N.; Fink, G. *Macromol. Chem.* **1992**, *193*, 773. (b) Coevoet, D.; Cramail, H.; Deffieux, A. *Macromol. Chem. Phys.* **1999**, *200*, 1208. (c) Chen, M. C.; Marks, T. J. *J. Am. Chem. Soc.* **2001**, *123*, 11803. (d) Busico, V.; Cipullo, R.; Cutillo, F.; Vacatello, M.; van Axel Castelli, V. *Macromolecules* **2003**, *36*, 4258.
(9) Chen, M. C.; Roberts, J. A.; Marks, T. J. *J. Am. Chem. Soc.* **2004**, *126*, 4605.
(10) Lancaster, S. J.; Walker, D. A.; Thornton-Pett, M.; Bochmann, M. *Chem. Commun.* **1999**, 1533.
(11) Song, F.; Cannon, R. D.; Bochmann, M. *J. Am. Chem. Soc.* **2003**, *125*, 7641.
(12) Lui, Z.; Somsook, E.; White, C. B.; Rosaaen, A.; Landis, C. R. *J. Am. Chem. Soc.* **2001**, *123*, 11193.
(13) (a) Beck, S.; Geyer, A.; Brintzinger, H. H. *Chem. Commun.* **1999**, 2477. (b) Beck, S.; Lieber, S.; Schaper, F.; Geyer, A.; Brintzinger, H. H. *J. Am. Chem. Soc.* **2001**, *123*, 1483. (c) Babushkin, D. E.; Brintzinger, H. H. *J. Am. Chem. Soc.* **2002**, *124*, 12869.
(14) (a) Stahl, N. G.; Zuccaccia, C.; Jensen, T. R.; Marks, T. J. *J. Am. Chem. Soc.* **2003**, *125*, 5256. (b) Zuccaccia, C.; Stahl, N. G.; Macchioni, A.; Chen, M. C.; Roberts, J. A.; Marks, T. J. *J. Am. Chem. Soc.* **2004**, *126*, 1448.
(15) Siedle, A. R.; Newmark, R. A. *J. Organomet. Chem.* **1995**, *497*, 119.
(16) Song, F.; Cannon, R. D.; Bochmann, M. *Chem. Commun.* **2004**, 542.
(17) Beswick, C. L.; Marks, T. J. *J. Am. Chem. Soc.* **2000**, *122,* 10358.

Scheme 1

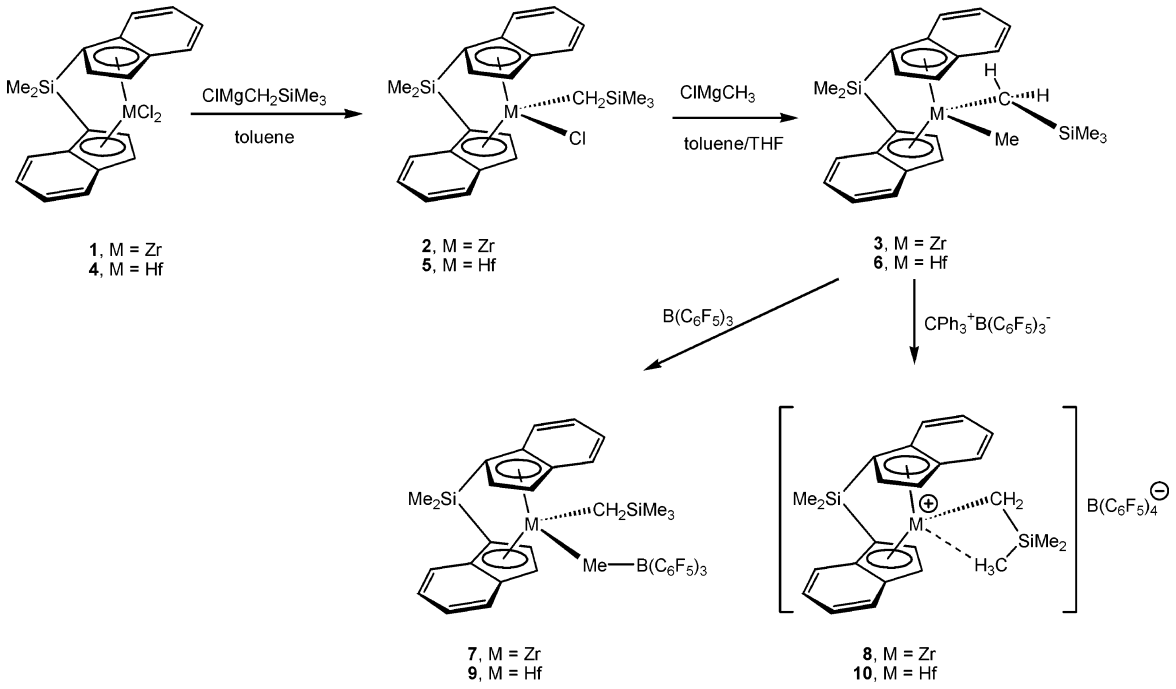

Scheme 2

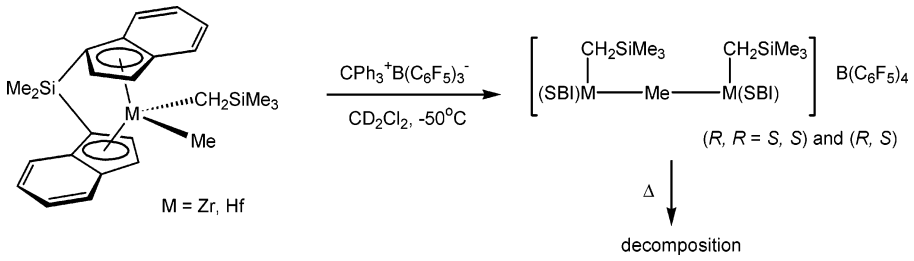

reotopic at room temperature, with one hydrogen experiencing significant high-field chemical shift due to the magnetic anisotropy of a neighboring indenyl ring, δ −2.07, −2.15, −2.05, and −2.20 for **2**, **3**, **5**, and **6** respectively, with geminal coupling constants $^2J_{HH} \approx$ 11.5 Hz.

Compound **3** reacts with $B(C_6F_5)_3$ exclusively with attack on the methyl ligand[17] to give (SBI)Zr(CH_2SiMe_3)(μ-Me)$B(C_6F_5)_3$ (**7**) (Scheme 1). The reaction is quantitative by NMR. Similarly, **3** reacts with CPh_3^+-$[B(C_6F_5)_4]^-$ in toluene or toluene/1,2-$C_6H_4F_2$ mixtures exclusively under methyl abstraction, to give the ion pair $[(SBI)ZrCH_2SiMe_3^+\cdots B(C_6F_5)_4^-]$ (**8**) as a red-orange solution. Attempted isolation of **8** resulted in the formation of a dark red-brown oil, which on prolonged evacuation gave a solid foam but no crystallizable product.

Attempts to generate $[(SBI)ZrCH_2SiMe_3^+\cdots B(C_6F_5)_4^-]$ in dichloromethane-d_2 solution at low temperature were unsuccessful. The initial product was a mixture of diastereomers of the homobinuclear methyl-bridged cation $[\{(SBI)ZrCH_2SiMe_3\}_2(\mu\text{-Me})][B(C_6F_5)_4]$, related to the previously characterized $[\{(SBI)ZrMe\}_2(\mu\text{-Me})][B(C_6F_5)_4]$.[18] In the presence of an excess of $CPh_3[B(C_6F_5)_4]$ this complex decomposed slowly to unidentified products (Scheme 2). The reaction in CD_2Cl_2 between $CPh_3[B(C_6F_5)_4]$ and excess **6** proceeded very slowly and required the sample to be warmed to a point at which rapid decomposition was apparent. ^{1}H NMR characterization of the diastereomeric pair of homobinuclear methyl-bridged cations $[\{(SBI)HfCH_2SiMe_3\}_2(\mu\text{-Me})][B(C_6F_5)_4]$ was achieved by performing the reaction in bromobenzene-d_5 at −10 °C, although even under these conditions the binuclear complex slowly decomposed to give the short-lived monomeric cation and subsequent unidentified products.

As in the neutral mixed-alkyl complex **3**, the Zr−CH_2 groups in the ion pairs are diastereotopic, although **8** shows a much larger chemical shift difference ($\Delta\delta$ = 2.81 at 25 °C, ^2J = 12.3 Hz; toluene-d_8/$C_6H_4F_2$, 9:1) than **7** ($\Delta\delta$ = 0.55, ^2J = 10.2 Hz, toluene-d_8, 25 °C). This reflects differences in the alkyl ligand bonding mode and anion binding, as shown below.

The diastereotopic character of the M-CH_2 moiety is borne out by the crystal structures of **3** and **6**. Both compounds are isostructural; the hafnium complex is shown in Figure 6. The crystal of **3** selected for X-ray diffraction from the first crystallization fraction turned out to be a product of cocrystallization of **2** and **3**, with disorder in the Zr-Me position; this was modeled with variable site occupancy which refined to $(CH_3)_{0.68}Cl_{0.32}$. In both compounds one of the methylene-hydrogen

(18) (a) Bochmann, M.; Jaggar, A. J. *J. Organomet. Chem.* **1992**, *424*, C5. (b) Bochmann, M.; Lancaster, S. J. *Angew. Chem., Int. Ed. Engl.* **1994**, *33*, 1634. (c) Bochmann, M.; Lancaster, S. J *J. Organomet. Chem.* **1995**, *497*, 55.

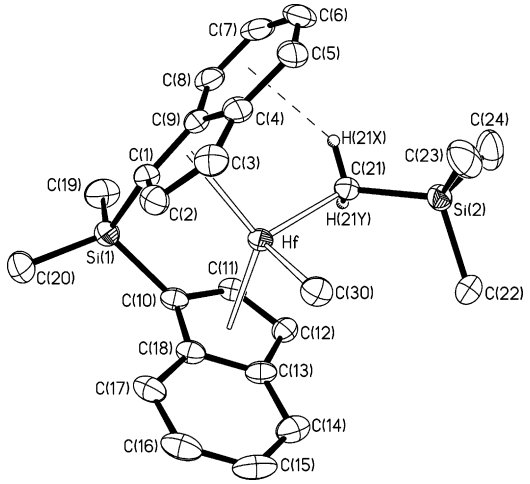

Figure 1. Molecular structure of (SBI)Hf(Me)CH_2SiMe_3 (**6**). Selected bond distances (Å) and angles (deg): Hf−C(21) 2.234(3); Hf−C(30) 2.239(3); H(21x)−C_6 centroid 2.35(4); Hf−Ct(1) 2.244; Hf−Ct(2) 2.244, where centroids Ct(1) and Ct(2) refer to rings C(1)−C(2)−C(3)−C(4)−C(9) and C(10)−C(11)−C(12)−C(13)−C(18), respectively; Ct(1)−Hf−Ct(2) 127.3; Ct(1)−Hf−C(21) 107.6; Ct(1)−Hf−C(30) 104.9; Ct(2)−Hf−C(21) 108.2; Ct(2)−Hf−C(30) 104.1; C(21)−Hf−C(30) 101.76(12); Hf−C(21)−Si(2) 122.5(2); C(1)−Si(1)−C(10) 96.64(14).

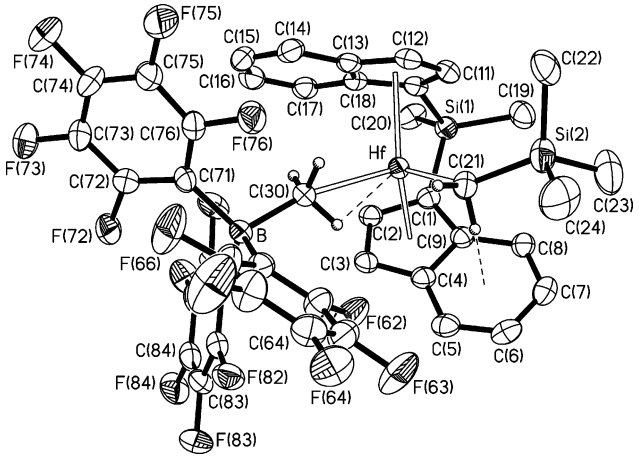

Figure 2. Molecular structure of (SBI)Hf(CH_2SiMe_3)(μ-Me)$B(C_6F_5)_3$ (**9**). Selected bond distances (Å) and angles (deg): Hf−C(21) 2.205(5); Hf−C(30) 2.546(5); C(30)−B 1.695(8); C(61)−B 1.649(8); C(21)−Si(2) 1.882(6); Hf−H(30a) 2.19; H(21b)−C_6 centroid 2.43; Hf−Ct(1) 2.232; Hf−Ct(2) 2.197, where centroids Ct(1) and Ct(2) refer to rings C(1)−C(2)−C(3)−C(4)−C(9) and C(10)−C(11)−C(12)−C(13)−C(18), respectively; Ct(1)−Hf−Ct(2) 127.8; Ct(1)−Hf−C(21) 107.4; Ct(1)−Hf−C(30) 107.1; Ct(2)−Hf−C(21) 108.4; Ct(2)−Hf−C(30) 106.7; C(21)−Hf−C(30) 94.3(2); Hf−C(21)−Si(2) 142.6(3); C(1)−Si(1)−C(10) 93.8(2).

atoms, H(21x), points directly toward the center of one of the indenyl six-rings, in **6** at a distance of only 2.35 Å, while the distance of H(21y) and the indenyl centroid is ca. 3.7 Å. This conformation allows the bulky $SiMe_3$ group to occupy a sterically least hindered position at the front of the metallocene wedge, bent toward the methyl ligand C(30).

In **9**, too, one of the methylene hydrogen atoms of the CH_2SiMe_3 ligand points toward the center of an indenyl six-ring, at a distance of 2.44 Å, although here the alkyl ligand adopts a different conformation from that in **6**, with the $SiMe_3$ group rotated away from the $MeB(C_6F_5)_3$ anion (Figure 2). The compound crystallizes with 1.5 toluene. Attempts to refine the H atoms on C(30) and C(21) freely failed, and the refinement became unstable; they were therefore inserted in idealized positions. As has been seen in other $MeB(C_6F_5)_3$ complexes,[19,20] anion binding involves agostic interactions with the metal center, in this case with H(30a), which shows a H···Hf distance of 2.19 Å. This is slightly shorter than the agostic Hf···H distances of 2.26(3) and 2.33(3) Å in the isoelectronic zwitterion Cp″Hf(η^3-C_3H_5){ η^1:η^3-CH_2C(Me)C(Me)$CH_2B(C_6F_5)_3$} (Cp″ = 1,3-$C_5H_3(SiMe_3)_2$).[21]

The $B(C_6F_5)_4^-$ ion pairs possess a rather different structure. Although, unsurprisingly, these complexes did not crystallize, the main structural features can be deduced from NMR spectroscopy and are shown particularly clearly in the case of the hafnium complex **10**. The chemical shift difference of the Hf-CH_2 signals ($\Delta\delta$ = 2.30 at 25 °C, ^2J = 12.6 Hz; toluene-d_8/$C_6H_4F_2$, 9:1) is similar to that of the Zr analogue **8**; the large $\Delta\delta$ value of the CH_2 group is reminiscent of that found with η^2-benzyl ligands[1c,20,22] and suggests a degree of conformational rigidity. At 20 °C the $SiMe_3$ signal is observed as a rather broad singlet, and cooling to −20 °C results in the splitting of this signal into two components in a ratio of 1:2, at δ −1.75 and −0.06, respectively (Figure 3), with further splitting of the more intense signal into two components becoming evident. Clearly the rotation of the $SiMe_3$ is slowed by an agostic interaction of one of the methyl groups with the metal center. In the case of the zirconium complex **8** such an interaction is weaker; cooling to −80 °C results in a broad $SiMe_3$ signal, although at 300 MHz the coalescence temperature could not be reached. The broadening, together with the large $\Delta\delta(CH_2)$ value of 2.81 referred to above, is in agreement with an alkyl ligand conformation similar to that found in **10**. This type of metal−silyl interaction is absent in the $MeB(C_6F_5)_3$ complexes **7** and **9**. It seems therefore that while in these $MeB(C_6F_5)_3$ complexes agostic interactions involve the anion-CH_3 group but not the alkyl ligand, the analogous $B(C_6F_5)_4^-$ complexes prefer η^2-type alkyl bonding via a γ-CH_3 group.

Such an alkyl bonding mode raises questions as to the nature of anion−cation interaction in such complexes. Although coordination of perfluorophenylborates via *o*-F and *m*-F close contacts has been crystallographically demonstrated for Cp*$_2$ZrH($HB(C_6F_5)_3$)[23] and Cp*$_2$-ThMe($B(C_6F_5)_4$),[5a] i.e., in the case of small σ-ligands and/or large metal centers, the steric requirements of an η^2-bonded bulky alkyl ligand would seem to leave little room for such anion coordination. The differences in alkyl bonding modes in compounds **7** and **10** are illustrated in Scheme 3. Since in structure **B** there are

(19) Yang, X.; Stern, C. L.; Marks, T. J. *J. Am. Chem. Soc.* **1994**, *116*, 10015.
(20) Bochmann, M.; Lancaster, S. J.; Hursthouse, M. B.; Malik, K. M. A. *Organometallics* **1994**, *13*, 2235.
(21) Jimenez-Pindado, G.; Thornton-Pett, M.; Bochmann, M. *J. Chem. Soc., Dalton Trans.* **1997**, 3115.
(22) (a) Bochmann, M.; Lancaster, S. J. *Organometallics* **1993**, *12*, 633. (b) Bochmann, M.; Lancaster, S. J. *Makromol. Chem. Rapid Commun.* **1993**, *14*, 807.
(23) Yang, X.; Stern, C. L.; Marks, T. J. *Angew. Chem., Int. Ed. Engl.* **1992**, *31*, 1375.

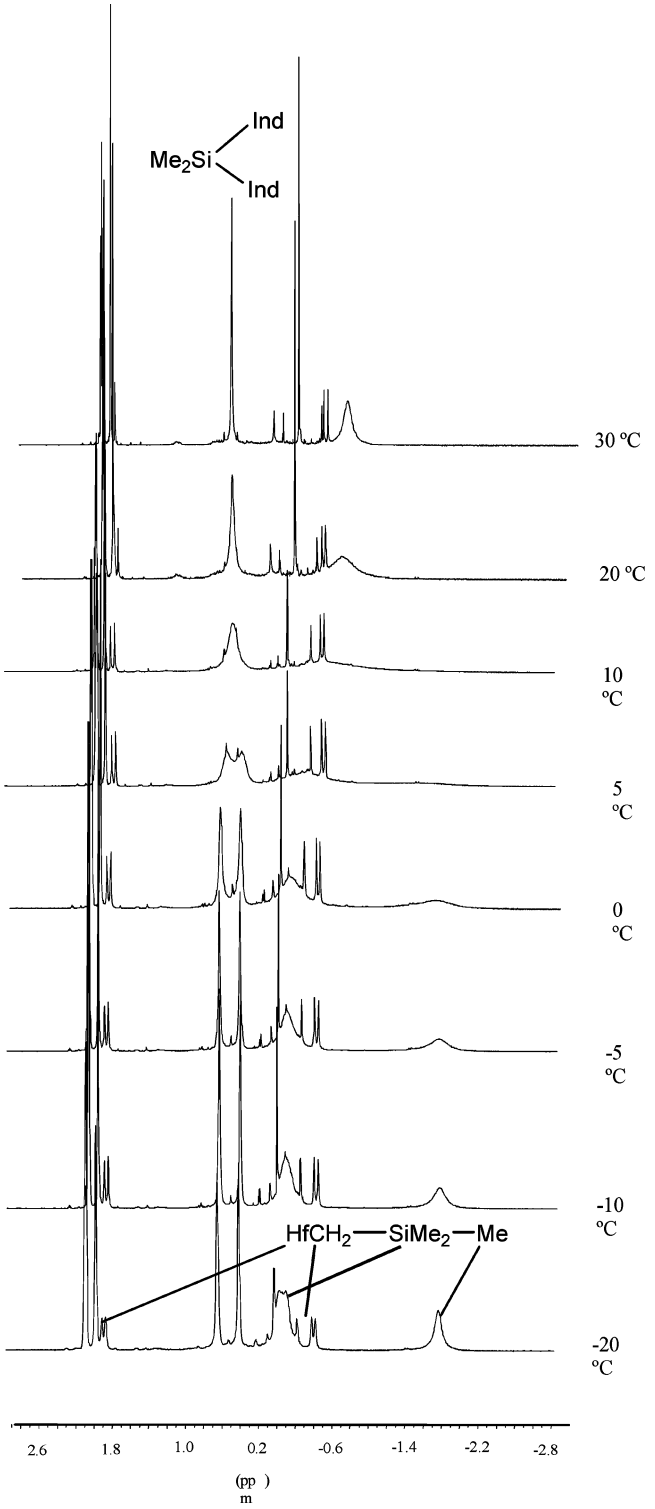

Figure 3. Variable-temperature ^{1}H NMR spectra of [(SBI)HfCH$_2$SiMe$_3^+$···B(C$_6$F$_5$)$_4^-$] (**10**) in toluene-d_8 with 10 vol % $F_2C_6H_4$.

no direct metal−fluorine contacts, the cation−anion interaction must be purely electrostatic. In effect, agostic alkyl bonding enforces an outer-sphere ion pair (OSIP) structure.

Related cases of stabilization by agostic interactions with silyl substituents have been reported, for example in [(1,2-C$_5$H$_3$Me$_2$)$_2$Zr(CH(SiMe$_3$)$_2$)][MeB(C$_6$F$_5$)$_3$][17] and in the crystallographically characterized zirconium vinyl complex [*rac*-C$_2$H$_4$(Ind)$_2$Zr(C(SiMe$_3$)=CMe$_2$][B(C$_6$H$_4$F)$_4$].[24] The activation barrier for silyl rotation in the latter case, $\Delta G^{\ddagger} = 10.7$ kcal mol^{-1} at −15 °C, is slightly lower than in **10** ($\Delta G^{\ddagger} = 12.6$ kcal mol^{-1} at 10 °C). Even though Horton's vinyl complex is somewhat more rigid and slightly more bulky than the CH$_2$SiMe$_3$ compounds under discussion here, it does provide a useful model for the relative positions of cations and anions in such species. Inspection of its unit cell gives the closest distances between the metal center and the nearest atoms of the anions, i.e., the *p*-F atoms, as 6.050 and 6.966 Å, with a closest Zr−B distance of 11.89 Å. With such long-range interactions, anion positions in solutions of compounds such as **8** and **10** are unlikely to be well-defined and are certainly not within bonding range.

Scheme 3

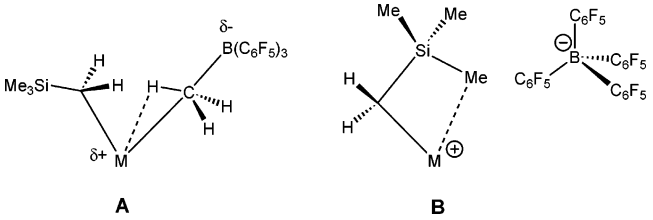

Ion Aggregation in Solution. To determine the influence of bulky alkyl chains on the tendency of such compounds to form ion aggregates, compounds **7** and **8** were investigated in solution by means of pulsed field-gradient spin−echo (PGSE)[25,26] and NOE[27,28] NMR experiments, respectively. The translational self-diffusion coefficient D_t is related to the hydrodynamic radius (r_H) of the diffusing particles according to a modified Stokes−Einstein equation: $D_t = kT/c\pi\eta r_H$ (where k is the Boltzmann constant, T is the temperature, c is a numerical factor that can be expressed as a function of r_H and the van der Waals radius of the solvent,[29] and η is the solution viscosity). From the experimentally determined D_t values, r_H, the hydrodynamic volumes (V_H), and c factors of the species present in solution were estimated. The ratio between V_H and the van der Waals volume of a single ion pair (V_{vdW}) afforded the aggregation number (N). The data are reported in Table 1. Toluene-d_8, the volume of which is excellently reproduced in a test experiment (entry 1), was used as internal standard to take into account changes in the solution viscosity due to the presence of small amounts of 1,2-difluorobenzene, as well as the relatively high concentration.

(24) Horton, A. D.; Orpen, A. G. *Organometallics* **1991**, *10*, 3910.
(25) Reviews on the PGSE NMR experiments: Johnson, C. S., Jr. *Prog. Nucl. Magn. Reson. Spectrosc.* **1999**, *34*, 203. Price, W. S. *Concepts Magn. Reson.* **1997**, *9*, 299. Price, W. S. *Concepts Magn. Reson.* **1998**, *10*, 197. Stilbs, P. *Prog. Nucl. Magn. Reson. Spectrosc.* **1987**, *19*, 1.
(26) Reviews on the application of PGSE NMR experiments to organometallic adducts: Binotti, B.; Macchioni, A.; Zuccaccia, C.; Zuccaccia, D. *Comments Inorg. Chem.* **2002**, *23*, 417. Macchioni, A. In *Perspectives in Organometallic Chemistry*; Screttas, C. G., Steele B. R., Eds.; The Royal Society of Chemistry: Cambridge, 2003; pp 196−207. Pregosin, P. S.; Martinez-Viviente, E.; Kumar, P. G. A. *Dalton Trans.* **2003**, 4007.
(27) Neuhaus, D.; Williamson, M. *The Nuclear Overhauser Effect in Structural and Conformational Analysis*; Wiley-VCH: New York, 2000.
(28) A review on the application of NOE experiments to investigate organometallic ion pairs: Macchioni, A. *Eur. J. Inorg. Chem.* **2003**, 195.
(29) Gierer, A.; Wirtz, K. *Z. Naturforsch. A* **1953**, *8*, 522. Spernol, A.; Wirtz, K. *Z. Naturforsch. A* **1953**, *8*, 532. Espinosa, P. J.; de la Torre, J. G. *J. Phys. Chem.* **1987**, *91*, 3612. Chen, H.-C.; Chen, S.-H. *J. Phys. Chem.* **1984**, *88*, 5118.

Table 1. Diffusion Coefficients D_t (10^{-10} m^2 s^{-1}), Hydrodynamic Radii r_H (Å), Hydrodynamic Volumes V_H (Å^3), *c* Factors, and Aggregation Numbers *N* for Solution of Compounds 7 and 8 at *C* Concentration (mM)

entry		*C* (mmol L^{-1})	D_t	r_H	*c*	V_H	*N*
1	toluene-d_8		21.7	2.74	3.5	86	0.99
2	[(SBI)Zr(CH_2SiMe_3)····$MeB(C_6F_5)_3$] (**7**)[a]	10	7.13	5.60	5.2	735	1.18
3	[(SBI)Zr(CH_2SiMe_3)$^+$····$B(C_6F_5)_4^-$] (**8**)[a]	10	4.64	8.01	5.6	2151	3.12
4	[(SBI)Zr(CH_2SiMe_3)$^+$····$B(C_6F_5)_4^-$] (**8**)[b]	1.6	5.64	6.78	5.5	1304	1.89

[a] Toluene-d_8/1,2-difluorobenzene, 9:1 vol:vol. [b] Toluene-d_8. The actual concentration (nominally 2 mM) was evaluated by integration relative to an external standard ($Si(SiMe_3)_4$ in toluene-d_8).

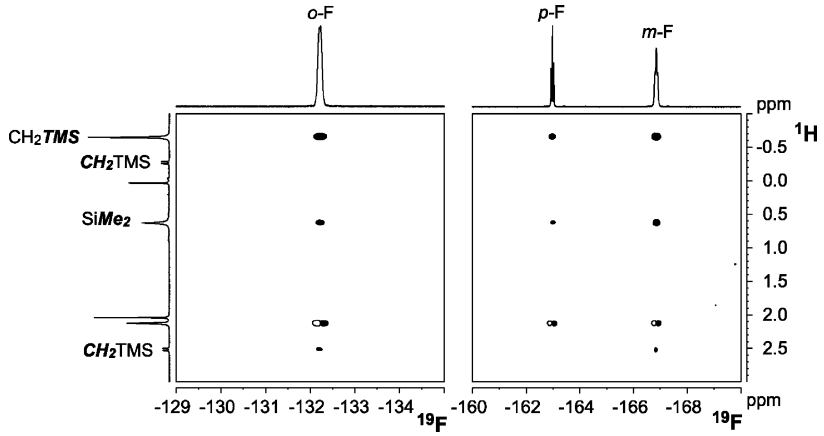

Figure 4. Two sections of the $^{19}F,^1H$ HOESY spectrum of a solution of **8** in toluene/$C_6H_4F_2$, 9:1 (10 mM), recorded at 295 K, showing interactions of the alkyl-$SiMe_3$ moiety and the $SiMe_2$ bridge with *o*-F (A) as well as *m*-F and *p*-F atoms of the $B(C_6F_5)_4$ anion (B) (relaxation delay = 1 s, mixing time = 0.5 s).

The apparent hydrodynamic volume of complex **7** (735 Å^3) in a solution of toluene-d_8/1,2-difluorobenzene, 9:1 (entry 2), is consistent with the predominant presence of single ion pairs (inner-sphere ion pairs). $^{19}F,^1H$ HOESY NMR investigations show that the anion binds to the cation in the usual fashion with the B−Me vector pointing toward the Zr center. In agreement with this structure, only the *o*-F fluorine nuclei interact with the CH_2SiMe_3 signal at −0.72 ppm (unfortunately, in this mixture of solvents, the resonance of one of the two diastereotopic CH_2SiMe_3 protons is obscured by the B*Me* resonance at −0.22 ppm) and with the CH_2SiMe_3 resonance, while both the *m*-F and *p*-F nuclei give a weak interaction with the CH_2SiMe_3 signal. From these observations we can conclude that the CH_2SiMe_3 ligand is preferentially oriented in such a way that the bulky $SiMe_3$ group is pointing away from the anion. In agreement with this bonding model, HOESY contacts between the fluorine nuclei and the protons of the Si*Me*$_2$ bridge were not observed.[30]

The apparent hydrodynamic volume of complex **8** in a solution of toluene-d_8/1,2-difluorobenzene, 9:1, is remarkably high (entry 3, 2151 Å^3) and suggests the presence of ion hextuples (aggregation number N = 3.12). This observation is consistent with the notion that **8** has a significantly stronger ionic character than **7**, a consequence of the relegation of the anion into the second coordination sphere caused by the $ZrCH_2Si(\kappa\text{-}Me)Me_2$ γ-agostic interaction illustrated in Scheme 3B. As a consequence, compound **8** has an increased tendency to form aggregates higher than simple ion pairs in low-polarity solvents.[14b] Sections of the $^{19}F,^1H$ HOESY experiments carried out for complex **8** at 295 K are shown in Figure 4. In contrast to **7**, not only the *o*-F but also the *m*-F and the *p*-F nuclei show dipolar interactions with the cationic moiety. In addition, interionic NOEs are now present between the anion and the Si*Me*$_2$ group of the backbone. Interestingly, the *CH*$_2$-$SiMe_3$ signal at δ −0.27 does not show any dipolar interaction with fluorine nuclei of the anion. While it seems possible to explain these observations by assuming that the anion pairs with the cation from both "lateral" sides, partly shifted toward the region of the space not occupied by the benzene rings of the indenyl ligands, it is not easy to combine this interpretation with the presence in solution of ion-hextuples as asserted by PGSE measurements.

Lowering the temperature from 295 to 217 K resulted in the precipitation of the well-known "oily" phase. Nevertheless, the total concentration in solution was still high enough to perform $^{19}F,^1H$ HOESY investigations.[31] The results are exemplified in Figure 5. The main difference with respect to the experiments recorded at 295 K is that now both the *CH*$_2$$SiMe_3$ protons seem to interact with the anion.

Finally, an apparent hydrodynamic volume of 1304 Å^3 (entry 4) was measured for a saturated solution of compound **8** in toluene-d_8 (1.6 mM). At this concentration, **8** exists predominantly as ion quadruples. The aggregation number N = 1.89 is in agreement with those reported earlier for donor-ligand-stabilized outer-sphere ion pairs.[14b]

Ion Pair Dynamics. Compounds **7**−**10** show fluxional behavior in solution, due to the site epimerization schematically depicted in Scheme 4. The process is

(30) It could be argued that the lack of this NOE is due to the fast relaxation of the two $SiMe_2$ resonances, but T_1 measurement by standard inversion recovery shows the following values: $SiMe_2$ (0.57 ppm), 0.810 s; $SiMe_2$ (0.425 ppm), 0.820 s; CH_2SiMe_3 (−0.077 ppm), 1.19 s; *CH*$_2$$SiMe_3$ (−0.22 ppm), 0.460 s.

(31) We believe that at this temperature the product $\omega\tau_c$ is bigger than 1.12 and that the negative NOE regime is reached, affording a higher sensitivity.

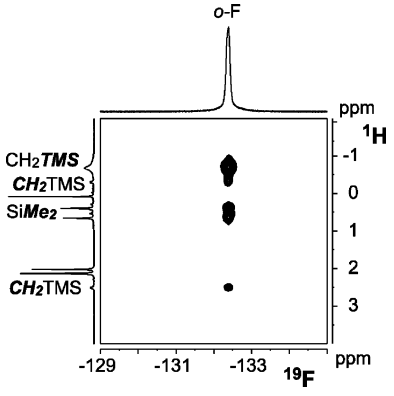

Figure 5. Section of the $^{19}F,^{1}H$ HOESY spectrum of a solution of **8** in toluene/$C_6H_4F_2$, 9:1, recorded at 217 K showing the interactions of both CH_2TMS protons with *o*-F.

Scheme 4

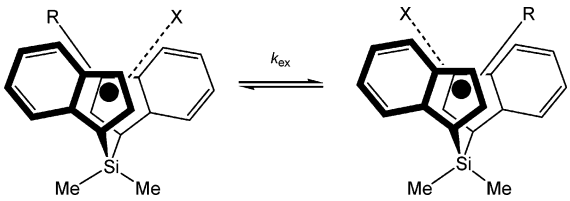

conveniently followed by variable-temperature ^{1}H NMR spectroscopy, using the $SiMe_2$ and indenyl-hydrogens in 2- and 3-position as reporter signals. In the MeB$(C_6F_5)_3^-$ complex **7**, the bridge-$SiMe_2$ signals coalesce at a comparatively high temperature, 40 °C, and are clearly resolved into two peaks at 10 °C (Figure 6). Unlike the related methyl complex (SBI)ZrMe(μ-Me)B$(C_6F_5)_3$, there is no possibility of a competing pathway involving symmetrization by dissociation of $B(C_6F_5)_3$.

The Zr-CH_2 moiety of **7** appears as two doublets with a chemical shift difference of $\Delta\delta = 1.1$ ppm, which is essentially independent of temperature. By contrast, for the Hf analogue **9** this chemical shift difference is much smaller and decreases on warming from $\Delta\delta = 0.59$ at −50 °C to $\Delta\delta = 0.2$ at 26 °C. While the spectrum at −5 °C shows the expected AB pattern, at 26 °C the low-field doublet of this group of resonances broadens, while its neighbor is unaffected (Figure 7). This effect is likely due to anion mobility, although the precise nature of this process could not be elucidated.

Compound **8** shows significantly faster site exchange than **7**, and coalescence of the $SiMe_2$ signals is reached at 0 °C. A stacked plot of the relevant sections of the variable-temperature ^{1}H NMR spectra of **8** is shown in Figure 8.

The data provide an interesting illustration of the stereochemistry of chain swinging. Thus while the bridge-$SiMe_2$ signals show the typical pattern for two-site exchange expected for this symmetrization process, the Zr-CH_2 signals remain unaffected and appear as an AB pattern throughout the observed temperature range; that is, the methylene hydrogens H^a and H^b do not interchange. This behavior is consistent with a chain swinging mechanism that involves a 180° rotation of the alkyl ligand (Scheme 5), as is indeed required by symmetry in a system with a C_2-symmetric ligand framework.

Ion pair symmetrization rate constants k_{ex} were calculated by comparison with simulated spectra.

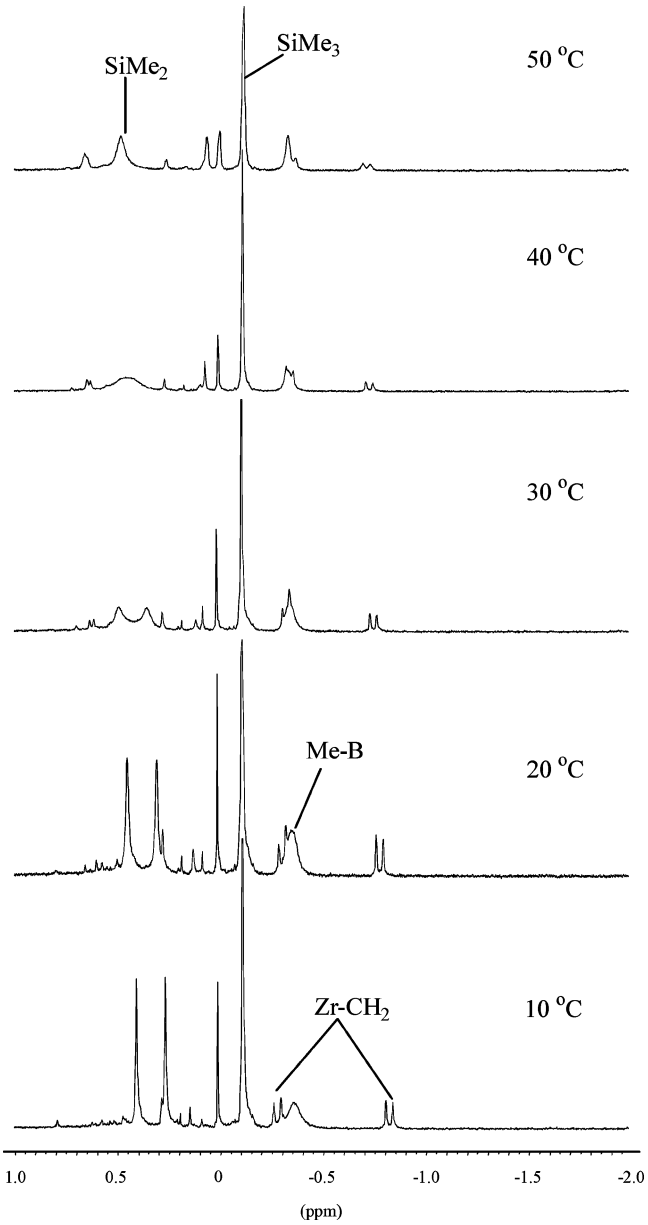

Figure 6. ^{1}H NMR spectra of (SBI)Zr(CH_2SiMe_3)(μ-Me)B$(C_6F_5)_3$ (**7**) in toluene-d_8; [Zr] = 2 mM.

Brintzinger et al. reported anion exchange parameters for the methyl complexes (SBI)ZrMe(μ-Me)B$(C_6F_5)_3$ (**11**) and [(SBI)ZrMe$^+\cdots$B$(C_6F_5)_4^-$] (**12**);[13b] these compounds were therefore included in our studies for comparison. The apparent first-order rate constants obtained by the spectra simulation method are in good agreement with Brintzinger's data derived from 2D-NOESY NMR techniques for a range of zirconium concentrations under essentially identical conditions (Table 2).

The data in Table 2 show several trends.

(1) The slow catalyst **11** gives k_{ex} values on the order of 2−5 s^{-1}. Replacement of the methyl ligand by the bulkier CH_2SiMe_3 ligand leads to a significant acceleration of k_{ex} in both the MeB$(C_6F_5)_3^-$ and B$(C_6F_5)_4^-$ compounds, evidently as the result of weakening the metal−anion interaction by steric pressure. The exchange rates for **7** and **9** are 5−10 times higher than for **11**.

A similar trend has been observed recently by Beswick and Marks for the series (1,2-$C_5H_3Me_2)_2$ZrR-

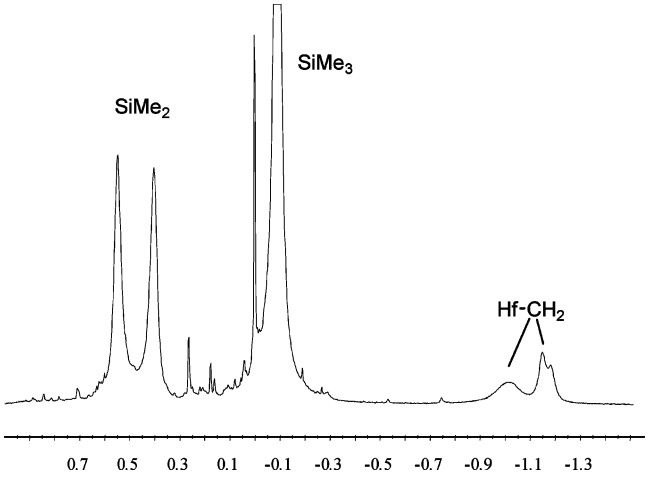

Figure 7. Hf-CH_2 and silyl region of the ^{1}H NMR spectrum of **9** in toluene-d_8 at 26 °C, showing the broadening of one doublet of the methylene AB pattern.

(μ-Me)B(C_6F_5)$_3$ (R = Me, CH_2CMe_3, CH_2SiMe_3, CH($SiMe_3$)$_2$).[17] The activation enthalpy for the site epimerization process (cf. Scheme 4) for **7**, $\Delta H^{\ddagger}_{ex} \approx 19$ kcal mol^{-1}, is comparable to that reported for (1,2-$C_5H_3Me_2$)$_2$-$ZrCH_2SiMe_3$(μ-Me)B(C_6F_5)$_3$ of 17(1) kcal mol^{-1}. The other compounds studied here have lower activation enthalpies (Table 3). Note that $\Delta H^{\ddagger}_{ex}$ is lowest for the hafnium complex **10**, for which agostic interactions with the alkyl ligand are strongest, although the strongly negative activation entropy ensures a slower exchange than is observed for zirconium.

(2) The rate of site epimerization ("chain swinging") of $B(C_6F_5)_4^-$ ion pairs increases with increasing metallocene concentration. This is in line with earlier observations by Brintzinger et al. on zirconocene methyl ion pairs,[13b] as well the finding that at the concentrations used for NMR experiments ([Zr] = 10^{-2}–10^{-3} mol L^{-1}) the $B(C_6F_5)_4^-$ compounds exist as ion aggregates in which distinct relative positions of anions and cations cannot be readily assigned and in which exchange of such loosely associated anions is facilitated. On the other hand, extrapolation of this trend to concentrations typically employed under catalytic conditions, i.e., [Zr] $\approx 10^{-5}$–10^{-6} mol L^{-1}, would suggest that the anion exchange rates observed here represent upper limits and that site epimerization at catalytic concentrations is in fact much slower.

(3) The more covalent $MeB(C_6F_5)_3^-$ complexes show no ($ZrCH_3$) or only a small (MCH_2SiMe_3) concentration dependence of k_{ex}, although this depends on the solvent.

(4) The exchange processes in $B(C_6F_5)_4^-$ compounds are up to 2 orders of magnitude faster than those in $MeB(C_6F_5)_3^-$ analogues. This trend reflects the well-established differences in catalytic activity between the two types of anions. Hafnium compounds exchange more slowly than zirconium.

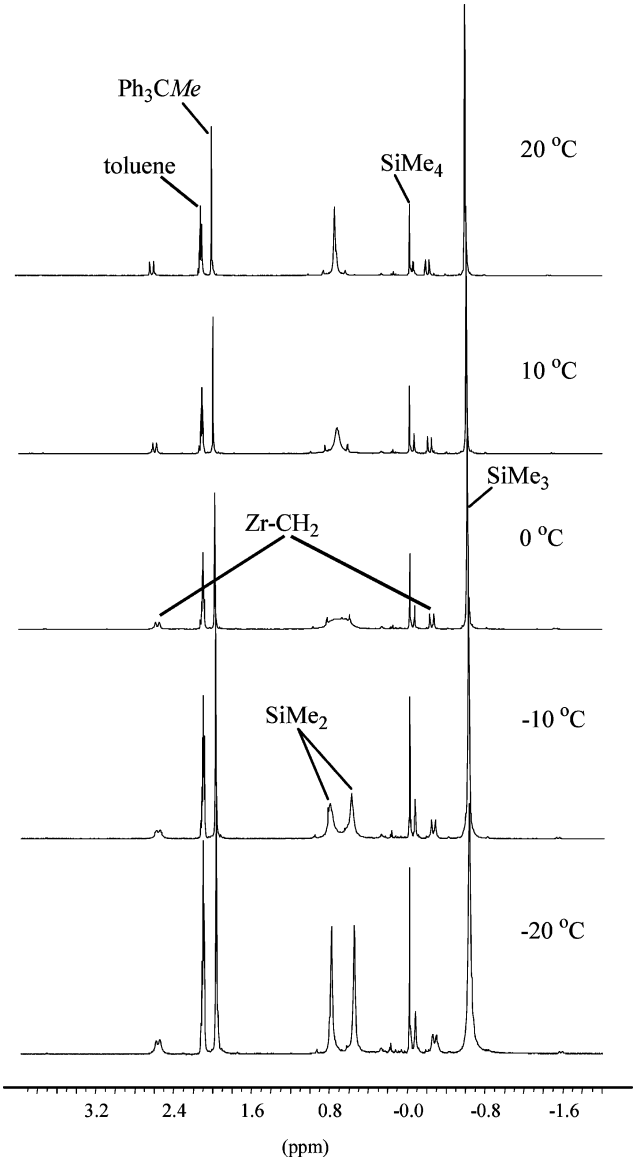

Figure 8. Variable-temperature ^{1}H NMR spectra of [(SBI)$Zr(CH_2SiMe_3)^+\cdots B(C_6F_5)_4^-$] (**8**) in toluene-$d_8$/1,2-$F_2C_6H_4$ (1:1); [Zr] = 20 mM.

(5) The exchange process is accelerated if the cosolvent 1,2-difluorobenzene is added to toluene. This solvent was required in the case of $B(C_6F_5)_4^-$ complexes at [metal] > 2 mM to ensure a homogeneous solution. Although the addition of a solvent with such a high dielectric constant (ϵ = 13.38) might be expected to facilitate solvation and anion dissociation, the effect is actually rather weak, with a 10-fold increase in [$C_6H_4F_2$] resulting in only a 2–3-fold increase in rate. As shown in the diffusion coefficient measurements, low concentrations (≤10 vol %) of $C_6H_4F_2$ do not in our view jeopardize the comparability of the data presented here.

Scheme 5

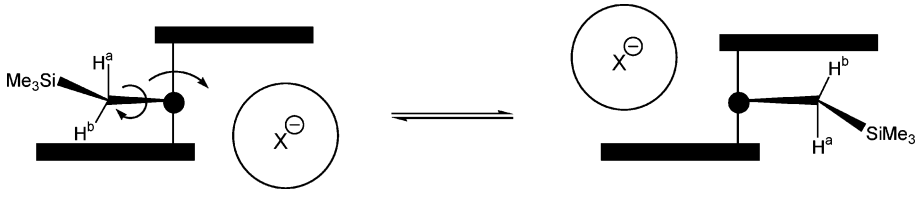

Table 2. Anion Exchange Rate Constant for [(SBI)MR$^+$X$^-$] (M = Zr, Hf; X = MeB(C$_6$F$_5$)$_3$ or B(C$_6$F$_5$)$_4$; R = Me, CH$_2$SiMe$_3$) in Toluene-*d*$_8$

compound	[metal] (mM)	$C_6H_4F_2$ cosolvent (vol %)	k_{ex} (s^{-1}) 20 °C	k_{ex} (s^{-1}) 25 °C	ref
[(SBI)ZrMe···MeB(C$_6$F$_5$)$_3$]	19	0		2.4 (27 °C)	*a*
	11.7	0	0	1.7 (27 °C)	*a*
	4	0	0	0.6 (27 °C)	*a*
[(SBI)ZrMe$^+$···B(C$_6$F$_5$)$_4^-$] [a]	1	0	178	288	*a*
[(SBI)ZrMe···MeB(C$_6$F$_5$)$_3$]	2	0	3 ± 0.6	4 ± 0.8	*b*
	20	10	4 ± 0.7	5 ± 0.8	
[(SBI)Zr(CH$_2$SiMe$_3$)···X]	2	0	14 ± 1	24 ± 1	*b*
X = MeB(C$_6$F$_5$)$_3$ **7**	2	10	12 ± 1	27 ± 2	
	20	0	18 ± 1	41 ± 3	
	20	10	60 ± 4	107 ± 8	
[(SBI)Zr(CH$_2$SiMe$_3$)···X]	2	~3	360 ± 100	500 ± 170	*b*
X = B(C$_6$F$_5$)$_4^-$ **8**	2	5	375 ± 65	540 ± 100	
	2	10	622 ± 100	980 ± 190	
	2	30	660 ± 80	1080 ± 180	
	20	50	1060 ± 250	1740 ± 480	
[(SBI)Hf(CH$_2$SiMe$_3$)···X]	2	0	21 ± 1.5	29 ± 3	*b*
X = MeB(C$_6$F$_5$)$_3^-$ **9**	20	0	31 ± 2	43 ± 3	
[(SBI)Hf(CH$_2$SiMe$_3$)···X]	2	10	180 ± 30	230 ± 50	*b*
X = B(C$_6$F$_5$)$_4^-$ **10**	20	10	330 ± 60	520 ± 110	

[a] Ref 13b. [b] This work.

Table 3. Activation Parameters for Site Epimerization Reactions of [(SBI)Zr(CH$_2$SiMe$_3$)···X] Ion Pairs in Toluene-*d*$_8$[a]

compound	[metal] (mM)	$C_6H_4F_2$ (vol %)	coalescence (°C)	$\Delta G^{\ddagger}_{ex}$[b] (kcal mol^{-1})	$\Delta H^{\ddagger}_{ex}$ (kcal mol^{-1})	$\Delta S^{\ddagger}_{ex}$ (cal mol^{-1} K^{-1})
[(SBI)Zr(CH$_2$SiMe$_3$)···X] X = MeB(C$_6$F$_5$)$_3$ **7**	2	0	40	15	19	10
[(SBI)Zr(CH$_2$SiMe$_3$)···X] X = B(C$_6$F$_5$)$_4^-$ **8**	2	3	5	13	11	−10
	2	30	5	13	15	8
[(SBI)Hf(CH$_2$SiMe$_3$)···X] X = MeB(C$_6$F$_5$)$_3^-$ **9**	2	0	45	16	10	−19
[(SBI)Hf(CH$_2$SiMe$_3$)···X] X = B(C$_6$F$_5$)$_4^-$ **10**	2	10	10	14	8	−21

[a] Cosolvent 1,2-difluorobenzene required for solubility as indicated. [b] Calculated at the coalescence temperature.

Scheme 6

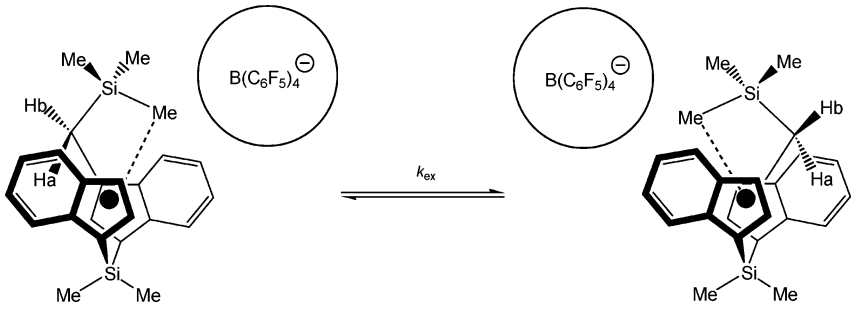

(6) Site epimerization is comparable to or slower than chain propagation. In fact, in only a few cases, such as for the C_1-symmetric catalysts (Cp-Z-Ind)ZrR(X) (Z = CMe_2 or $SiMe_2$; X = MeMAO, MeB(C$_6$F$_5$)$_3$, or B(C$_6$F$_5$)$_4$) has site epimerization been shown to be significantly faster than chain propagation.[32]

Our results on metal−CH_2SiMe_3 complexes show that B(C$_6$F$_5$)$_4^-$ complexes carrying such bulky alkyl ligands do not form inner-sphere complexes. The NOE experiments suggest that the anion is located near the open wedge of the SBI ligand, such that interactions with the $SiMe_3$ and CH_2 moieties of the ligand are possible. Ion pair symmetrization in this case is envisaged to involve site exchange of the alkyl and the anion without direct metal−anion contact (Scheme 6).

Ion Pair Symmetrization Rates and Their Implications for Alkene Polymerization Kinetics. Ion pair symmetrization rates (here also referred to as anion exchange rates) are intimately connected with the alkene insertion process; both situations involve anion displacement, the first by solvent, the latter by the monomer.[33a] Chain growth involves two steps, monomer association (which, for MeB(C$_6$F$_5$)$_3^-$ compounds at least, involves anion substitution), followed by the migration of the polymeryl chain to the coordinated alkene. Theoretical modeling of this process using MeB(C$_6$F$_5$)$_3^-$

(32) Mohammed, M.; Nele, M.; Al-Humydi, A.; Xin, S.; Stapleton, R. A.; Collins, S. *J. Am. Chem. Soc.* **2003**, *125,* 7930.

(33) For recent theoretical models see for example: Chan, M. S. W.; Vanka, K.; Pye, C. C.; Ziegler, T. *Organometallics* **1999**, *18*, 4624. (b) Chan, M. S. W.; Ziegler, T. *Organometallics* **2000**, *19*, 5182. (c) Xu, Z. T.; Vanka, K.; Firman, T.; Michalak, A.; Zurek, E.; Zhu, C. B.; Ziegler, T. *Organometallics* **2002**, *21*, 2444. (d) Nifant'ev, I. E.; Ustynyuk, L. Y.; Laikov, D. N. *Organometallics* **2001**, *20*, 5375. (e) Lanza, G.; Fragalà, I. L.; Marks, T. J. *Organometallics* **2002**, *21*, 5594. (f) Xu, Z.; Vanka, K.; Ziegler, T. *Organometallics* **2004**, *23*, 104.

Table 4. Comparison of First-Order Rate Constants for Site Epimerization and Observed Propagation Rates for Propene Polymerizations[a]

compound	k_{ex}[a] (s^{-1})	k_p^{obs} [b] (s^{-1})	$k_p[C_3H_6]$[c] (s^{-1})	T (°C)	$[C_3H_6]$ (mol L^{-1})	ref
[(SBI)Zr(CH_2SiMe_3)···X] X = $MeB(C_6F_5)_3$ **7**	14 ± 1	14 ± 1		20	0.71	16
[(SBI)Zr(CH_2SiMe_3)···X] X = $B(C_6F_5)_4^-$ **8**	375 ± 65 500 ± 170	970 ± 10		20 25	0.71	16
(SBI)$ZrMe_2$/$AlBu^i_3$/$CPh_3[CN\{B(C_6F_5)_3\}_2]$		780 ± 13	10 120 ± 800	25	0.59	11
$Me_2Si(C_5Me_4)(NBu^t)TiCl_2$/$AlBu^i_3$/$CPh_3[B(C_6F_5)_4]$			11 400	25	0.59	38
rac-Me_2Si(2-Me-4,5-Benz[*e*]Ind)$_2ZrCl_2$/ $AlBu^i_3$/$CPh_3[B(C_6F_5)_4]$		8000		25	0.59	38

[a] This work; k_{ex} determined by VT-NMR. [b] $k_p^{obs} = k_p^{app}[M]$, from the rate law $-d[M]/dt = k_p^{app}[C_0][M]_0$, where $[C_0]$ = total catalyst concentration, $[M]_0$ = initial monomer concentration. [c] Determined from the time dependence of the number-average molecular weight.

Scheme 7

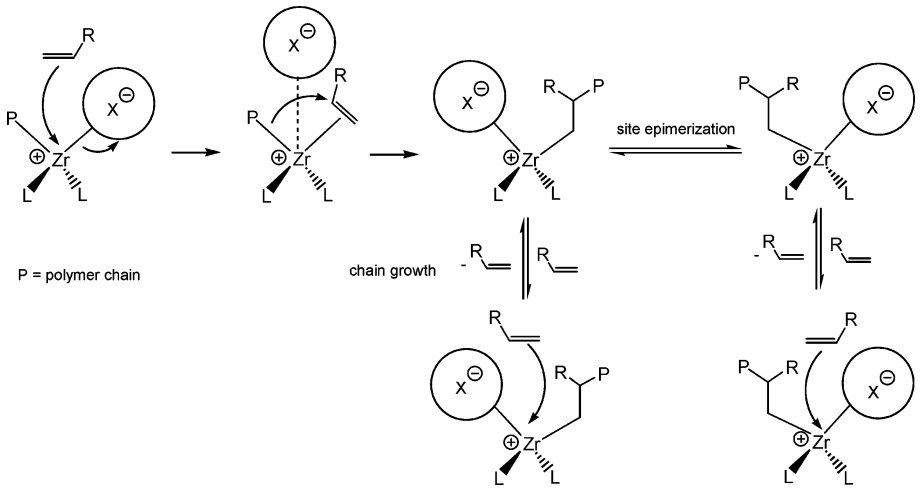

compounds has shown that the primary insertion product may be stabilized by reassociation of the anion in a site *cis* to its original position (Scheme 7).[33]

Opposing views have recently been expressed in the literature concerning the mechanism of alkene polymerization and the role of the counteranion. Early kinetic studies by Fink[34] on titanocene-catalyzed ethylene oligomerizations have led to a model where catalyst activation (by some chemical process such as anion displacement) is slow and is followed by the insertion of one or more monomer units, with chain growth being interrupted at any stage by the (reversible) stabilization of the product as a dormant state. Only the latter is spectroscopically observable. This model has become known as the "intermittent mechanism".[35] More recently, Brintzinger et al. studied the reactions of a series of zirconocene methylborates with weak donors such as di-*n*-butyl ether (DBE). The second-order rate constants for anion displacement k_{sub} changed by 5 orders of magnitude, depending on the ligand framework, though anion substitution was found to be slow for those complexes known to be the most effective catalysts for propene polymerization. However, the reverse reaction, the rate of displacement of DBE by $MeB(C_6F_5)_3^-$, was even slower. The authors suggested that these findings pointed toward a mechanism where chain growth was initiated by anion displacement and proceeded by successive rapid monomer enchainments, which were interrupted by slow anion recoordination.[36] On the other hand, Landis showed that in 1-hexene polymerizations with (EBI)$ZrMe_2$/$B(C_6F_5)_3$ at low temperature (EBI = *rac*-C_2H_4(1-Ind)$_2$), where the system is living and Zr-polymeryl species are directly NMR-observable, each monomer insertion was followed by anion reassociation in a concerted process. Here, propagation is thought to be initiated by displacement of the anion from the inner coordination sphere and reversible monomer association, followed by irreversible insertion and finally rapid anion recoordination to the metal center. This mechanism has been referred to as the "continuous" propagation mode[37] and corresponds to the chain growth steps depicted in Scheme 7.

Rates of ion pair symmetrization k_{ex} and the propagation rates for propene polymerizations with (SBI)Zr catalysts are collected in Table 4. As shown earlier,[11] for the (SBI)$ZrMe_2$/$AlBu^i_3$/$CPh_3[B(C_6F_5)_4]$ system the rate of growth of a polymer chain, as determined by the number-average molecular weight as a function of time during the initial phase of the polymerization, is about 1 order of magnitude faster than the propagation rate determined from the polymer yield. For the (SBI)Zr

(34) (a) Schnell, D.; Fink, G. *Angew. Makromol. Chem.* **1974**, *39*, 131. (b) Fink, G.; Zoller, W. *Makromol. Chem.* **1981**, *182*, 3265. (c) Fink, G.; Schnell, D. *Angew. Makromol. Chem.* **1982**, *105*, 31. (d) Mynott, R.; Fink, G.; Fenzl, W. *Angew. Makromol. Chem.* **1987**, *154*, 1. (e) Fink, G.; Fenzl, W.; Mynott, R. *Z. Naturforsch. Teil B* **1985**, *40b*, 158.

(35) For clarity it should be noted that although this model (ref 34) describes the fast buildup of polymer chains on a few centers while others remain inactive, dormant state formation is thought to be possible after *every* monomer insertion step. The model does not necessarily imply multiple monomer insertions or "bursts of propagation" (but see also refs 36 and 37).

(36) Schaper, F.; Geyer, A.; Brintzinger, H. H. *Organometallics* **2002**, *21*, 473.

(37) Landis, C. R.; Rosaeen, K. A.; Sillars, D. R. *J. Am. Chem. Soc.* **2003**, *125*, 1710.

Table 5. Crystal Data and Refinement Details

	3	**6**	**9**
formula	major component: $C_{25}H_{32}Si_2Zr$ minor component: $C_{24}H_{29}ClSi_2Zr$	$C_{25}H_{32}HfSi_2$	$C_{53}H_{44}BF_{15}HfSi_2$
fw	479.92; 500.34	567.18	1211.36
temp, K	140(1)	180(2)	180(2)
cryst syst	monoclinic	monoclinic	triclinic
space group	$P2_1/c$	$P2_1/c$	$P\bar{1}$
a, Å	14.403(3)	14.3497(2)	12.1423(2)
b, Å	12.499(3)	12.5146(2)	13.8662(2)
c, Å	13.997(3)	13.9676(2)	17.0088(3)
α, deg	90	90	106.0594(6)
β, deg	110.36(3)	110.2146(9)	100.7050(6)
γ, deg	90	90	108.0499(6)
V, Å^3	2362.3(8)	2353.81(6)	2498.38(7)
D_{calc}, g cm^{-3}	1.368	1.600	1.610
Z	4	4	2
μ, mm^{-1}	0.611	4.542	2.228
indep/obsd ($I > 2\sigma_I$) reflns	4297/4027	6300/5415	10 171/8679
no. of data/restraints/params	4297/0/267	6285[d]/0/262	10 171/0/643
F(000)	1010	1128	1204
R_{int}[a]	0.0279	0.0525	0.0571
R_1 [$I>2\sigma(I)$] [b]	0.0282	0.0282	0.0426
wR_2 (all data)[c]	0.0763	0.0763	0.1401
GOF on F^2	1.050	1.050	1.084

[a] $\sum|F_o^2 - F_o^2(mean)|/\sum F_o^2$. [b] $R_1 = \sum||F_o| - |F_c||/\sum|F_o|$. [c] $wR_2 = [\sum w(F_o^2 - F_c^2)^2/\sum w(F_o^2)^2]^{1/2}$; $w = [\sigma^2(F_o^2) + (aP)^2 + bP]^{-1}$, where $P = [2F_c^2 + \max(F_o^2, 0)]/3$. [d] 15 reflns were suppressed by the SHELXL program.

Scheme 8

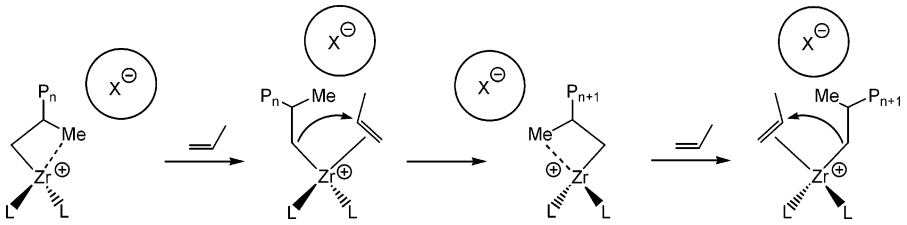

system, the growth rate of $\bar{M}_n$ at 25 ± 0.1 °C was estimated as $k_p^{obs} = k_p[M] \approx 10^4$ s^{-1} (under 1 bar propene; this value would rise to >10^5 s^{-1} in neat propene). Even higher propene propagation rates were found by quenched-flow kinetics for the constrained-geometry catalyst $Me_2Si(C_5Me_4)(NBu^t)TiCl_2/AlBu^i_3/CPh_3[B(C_6F_5)_4]$, as well as in batch reactions with *rac*-Me_2Si(2-Me-4,5-Benz[*e*]Ind)$_2ZrCl_2/AlBu^i_3/CPh_3[B(C_6F_5)_4]$;[38] these data are included for comparison.

The polymerization and site epimerization rates clearly fall into two categories. For $MeB(C_6F_5)_3^-$ complexes, both k_{ex} and k_p^{obs} are low and reflect a situation where anion displacement from the inner coordination sphere is rate limiting and the propagation process is as outlined for the "continuous" mechanism. Changing the anion to $B(C_6F_5)_4^-$ increases k_{ex} ~30-fold, while k_p^{obs} rises by up to 3 orders of magnitude. The reason for this rate increase is the outer-sphere structure of the $B(C_6F_5)_4^-$ ion pairs **8** and **10** discussed above: since the anion never enters the metal coordination sphere, anion displacement is not a major contribution to the activation barrier of monomer insertion. Although strictly speaking this situation has only been demonstrated here for CH_2SiMe_3 compounds, it seems reasonable to assume that other alkyl chains with methyl substituents in β-position, such as Zr−PP, will lead to similar β- or γ-agostically bonded ion pair structures.

We conclude therefore that while for $MeB(C_6F_5)_3^-$ complexes chain propagation follows an ISIP ("continuous") mechanism, high activity polymerization catalysts ($k_p \geq 10^4$ L mol^{-1} s^{-1}) operate under a different kinetic regime, without the need for anion displacement from the inner coordination sphere, and where monomer uptake is not impeded by competitive anion reassociation.

The structures of stable compounds such as **8** and **10** represent resting states, with the anion in an outer-sphere position. The reaction of such a species with the approaching monomer can be envisaged to involve a loosening of the agostic M···CH_3 interaction and a change in alkyl ligand conformation, likely accompanied by an increase in the metal−anion distance (Scheme 8). This process is "intermittent" in the sense that after each insertion step an agostically stabilized ion pair is formed. Thus these catalysts appear to comply with the original ionic model[1−3] based on "naked" metallocenium cations, with the refinement that in nonpolar media cations and anions do not diffuse freely and the ion pairs therefore exist as distinct compounds.

Conclusion

The readily accessible mixed-alkyl metallocene complexes (SBI)M(Me)CH_2SiMe_3 (M = Zr, Hf) provide a route to the ion pairs [(SBI)M$CH_2SiMe_3^+$···$B(C_6F_5)_4^-$]. These compounds are thermally remarkably stable in toluene solution. The β-methyl branched alkyl ligand acts as a model for ligated polypropylene and offers insight into the stereochemistry of chain swinging, with 180° rotation in C_2-symmetric catalysts, as well as the mode of alkyl bonding. Agostic bonding to β-methyl

(38) Song, F.; Cannon, R. D.; Lancaster, S. J.; Bochmann, M. *J. Mol. Catal. A: Chem.* **2004**, *218*, 21.

substituents is preferred over anion coordination, resulting in an outer-sphere ion pair structure. Site epimerization is faster than with Zr-CH_3 analogues. Rates decrease with decreasing metallocene concentration; the observed values therefore represent upper limits for the exchange rates expected for the low metal concentrations employed under catalytic conditions. At [metal] ≈ 2 mM, [(SBI)$ZrCH_2SiMe_3^+\cdots B(C_6F_5)_4^-$] exists as ion quadruples, while at 10 mM concentration the aggregation number rises to 3. It appears that chain propagation may follow two distinct intimate mechanisms, depending on the ability of the counteranion to act as inner-sphere ligand or not. For slow polymerizations and ISIP catalysts with $MeB(C_6F_5)_3^-$ as counteranion, the so-called "continuous" mechanism operates, consisting of an anion substitution−monomer insertion−anion recoordination reaction sequence. The structures of the catalytically much more active $B(C_6F_5)_4^-$ complexes, on the other hand, suggest that in these cases a different regime prevails where the anion does not directly coordinate to the metal and where propagation rates are not limited by ion separation. Agostic bonding as seen in **8** and **10** provides a facile stabilization mode of the active species as an outer-sphere ion pair resting state. It remains to be seen to what extent this alkyl bonding mode and ion pair structure applies to unbranched polymer chains, i.e., ethene polymerization systems.

Experimental Section

All manipulations were performed under dry nitrogen gas using standard Schlenk techniques. Solvents were purified by distillation under nitrogen from sodium−potassium alloy (light petroleum, bp 40−60 °C) or sodium (low-sulfur toluene) or sodium-benzophenone (THF). (SBI)$ZrCl_2$ (**1**),[39] (SBI)$ZrMe_2$,[20] and (SBI)$HfCl_2$[40] (SBI = *rac*-$Me_2Si(1\text{-Ind})_2$) were prepared according to literature methods and stored as solids in a drybox under nitrogen at room temperature. $CPh_3[B(C_6F_5)_4]$ was synthesized from Ph_3CCl with $Li[B(C_6F_5)_4]$ in dichloromethane and recrystallized from a dichloromethane/light petroleum mixture solvent to afford a yellow crystalline solid in 97% yield.[41] $Li[B(C_6F_5)_4]$ was made from $B(C_6F_5)_3$ and LiC_6F_5 in light petroleum and was free from other borate impurities within NMR detection limits (^{19}F, ^{11}B) without further purification. Deuterated toluene was dried by stirring over Na/K alloy at about 60 °C over 10 h followed by trap-to-trap distillation; 1,2-$C_6H_4F_2$ was degassed and dried over activated 4 Å molecular sieves.

NMR (^1H, ^{13}C, ^{19}F, ^{11}B) spectra were recorded on a Bruker Avance DPX-300 spectrometer. Chemical shifts were referenced to residual solvent peaks (^1H, ^{13}C), $CFCl_3$ (^{19}F), or $BF_3{\cdot}OEt_2$ (^{11}B). Variable-temperature NMR spectra of ion pairs were recorded at temperature intervals of 5 °C over a range from −20 to 10 °C (compounds **8** and **10**) and 0 to 40 °C (compounds **7** and **9**). Acquisition relaxation delay (D1) was 12 s and time domain size 65 536 data points. A total of 32−64 scans were accumulated (^1H). Spectra were simulated using the gNMR program (v. 4.1). Rate constants at each temperature were estimated by visual matching of line shapes of simulated and experimental spectra. Ion pair symmetrization rate constants for **8** and **10** at 20 and 25 °C were obtained by linear extrapolation of $\ln(k/T)$ vs $1/T$. For **7** and **9** rate constants at these temperatures were determined by regression analysis of the Eyring plot.

(SBI)Zr(Cl)CH_2SiMe_3 (2). (SBI)$ZrCl_2$ (1.1 g, 2.5 mmol) was suspended in 50 mL of toluene and was cooled to 0 °C. Me_3SiCH_2MgCl (2.45 mmol, 1.63 mL, 1.5 M in Et_2O) was slowly added, and the reaction mixture was stirred for 10 h at room temperature. Filtration and removal of volatiles gave **2** as an orange crystalline solid. ^1H NMR (300 MHz, 25 °C, C_7D_8): δ 7.53 (d, J = 8.6 Hz, 1H, C_6-Ind), 7.41 (d, J = 8.6 Hz, 1H, C_6-Ind), 7.27 (d, J = 8.6 Hz, 1H, C_6-Ind), 7.2−6.6 (m, 6H, C_6-Ind and C_5-Ind), 6.59 (d, J = 3.3 Hz, 1H, C_5-Ind), 5.87 (d, J = 3.3 Hz, 1H, C_5-Ind), 5.39 (d, J = 3.3 Hz, 1H, C_5-Ind), 0.59 (s, 3H, $SiMe_2$), 0.50 (s, 3H, $SiMe_2$), 0.32 (d, ^2J = 11.7 Hz, $ZrCH_2$), 0.14 (s, 9H, $SiMe_3$), −1.96 (d, ^2J = 11.7 Hz, $ZrCH_2$). ^{13}C NMR ($CDCl_3$): δ 58.2 ($ZrCH_2$), 2.4 ($SiMe_3$), −0.72 ($SiMe_2$), −1.77 ($SiMe_2$); indenyl signals omitted.

(SBI)Zr(Me)CH_2SiMe_3 (3). Method 1. To a solution of **2** from the above reaction in 50 mL of toluene was added ClMgMe (3.0 mmol, 1 mL, 3 M in THF) at room temperature. After 1 h, **2** was isolated from the filtrate as an orange solid, which was recrystallized from light petroleum. **Method 2.** To an orange suspension of **1** (5.2 g, 11.6 mmol) in 150 mL of toluene at −20 °C was added Me_3SiCH_2MgCl in Et_2O (11.7 mmol, 7.8 mL, 1.5 M). The reaction mixture was stirred for 1 h at −20 °C and for 16 h at room temperature and filtered. A solution of MeMgCl in THF was then added (12.0 mol, 4.0 mL, 3 M), and stirring was continued for 10 h. The first fraction consisted of cocrystals of **2** and **3** contaminated with some **2**, as evidenced by the X-ray analysis; the second crop consisted of pure **3** (by NMR) (4.1 g, 8.6 mmol, 74.1%). Anal. Calcd for $C_{25}H_{32}ZrSi_2$: C, 62.57; H, 6.72. Found: C, 61.93; H, 6.65. ^1H NMR (300 MHz, 25 °C, benzene-d_6): δ 7.56−7.49 (m, 2H, C_6-Ind), 7.19−7.10 (m, 4H, C_6-Ind), 6.88 (d, J = 3.0 Hz, 1H, C_5-Ind), 6.81−6.74 (m, 2H, C_6-Ind), 6.63 (d, J = 3.3 Hz, 1H, C_5-Ind), 5.65 (d, 1H, J = 3.3 Hz, C_5-Ind), 5.55 (d, J = 3.0 Hz, 1H, C_5-Ind), 0.53 (s, 3H, $SiMe_2$), 0.50 (s, 3H, $SiMe_2$), 0.06 (s, 9H, $SiMe_3$), −0.21 (d, 1H, ^2J = 11.4 Hz, $ZrCH_2$), −1.05 (s, 3H, ZrMe), −2.13 (d, 1H, ^2J = 11.4 Hz, $ZrCH_2$). ^{13}C NMR (75.47 MHz, 25 °C, benzene-d_6): δ 131.10, 130.04, 126.89, 125.87, 125.79, 125.33, 125.18, 125.09, 124.92, 124.33 (C_6-Ind), 117.76, 116.83, 113.64, 109.45, 86.36, 83.15 (C_5-Ind), 52.19 (J_{CH} = 107 Hz, $ZrCH_2$), 38.92 (J_{CH} = 119 Hz, ZrMe), 2.96 ($SiMe_3$), −1.42 ($SiMe_2$), −2.50 ($SiMe_2$).

(SBI)Hf(Cl)CH_2SiMe_3 (5). A suspension of (SBI)$HfCl_2$ (8.6 g, 16.0 mmol) in toluene (200 mL) was treated with $ClMgCH_2SiMe_3$ (32 mL, 1.2 M solution in Et_2O, 42 mmol). The mixture was warmed to 80 °C and stirred for 16 h. Removal of the volatiles under reduced pressure yielded a yellow solid. This residue was extracted with toluene (80 mL). Concentration and cooling to −25 °C yielded pale yellow crystals (two crops, 6.0 g, 10.2 mmol, 64%). Anal. Calcd for $C_{24}H_{29}ClHfSi_2$: C, 49.06; H, 4.97; Cl, 6.03. Found: C, 48.67; H, 4.79; Cl, 5.30. ^1H NMR (300 MHz, 25 °C, benzene-d_6): δ 7.53 (d, J = 8.6 Hz, 1H, C_6-Ind), 7.40 (d, J = 8.6 Hz, 1H, C_6-Ind), 7.35 (d, J = 8.7 Hz, 1H, C_6-Ind), 7.17−7.07 (m, 3H, C_6-Ind), 6.89−6.83 (m, 1H, C_6-Ind), 6.79 (d, J = 3.0 Hz, 1H, C_5-Ind), 6.77−6.71 (m, 1H, C_6-Ind), 6.52 (m, 1H, C_5-Ind), 5.88 (d, J = 3.3 Hz, 1H, C_5-Ind), 5.32 (d, J = 3.0 Hz, 1H, C_5-Ind), 0.58 (s, 3H, $SiMe_2$), 0.47 (s, 3H, $SiMe_2$), 0.18 (s, 9H, $SiMe_3$), −0.35 (d, ^2J = 12.1 Hz, $HfCH_2$), −2.05 (d, ^2J = 12.1 Hz, $HfCH_2$). ^{13}C NMR (75.47 MHz, 25 °C, benzene-d_6): δ 132.66, 130.72, 126.90, 126.37, 126.21, 125.79, 125.68, 125.51, 125.46, 124.10, 124.01 (C_6-Ind), 116.39, 115.49, 113.98, 111.23, 89.76, 87.31 (C_5-Ind), 53.59 (J_{CH} = 108 Hz, $HfCH_2$), 2.81 ($SiMe_3$), −1.53, −2.58 ($SiMe_2$).

(SBI)Hf(Me)CH_2SiMe_3 (6). A solution of ClMgMe in THF (1 mL, 3 M, 3 mmol) was added to a solution of (SBI)Hf(Cl)-CH_2SiMe_3 (1.1 g, 1.9 mmol) in toluene (20 mL). The resulting mixture was stirred overnight at room temperature before separating the suspended solids by filtration. Concentrating the solution and cooling to −25 °C gave pale yellow crystals

(39) Spaleck, W.; Antberg, M.; Rohrmann, J.; Winter, A.; Bachmann, B.; Kiprof, P.; Behm, J.; Herrmann, W. A. *Angew. Chem., Int. Ed. Engl.* **1992**, *31*, 1347.
(40) Nifant'ev, I. E.; Ivchenko, P. V. *Organometallics* **1997**, *16*, 713.
(41) (a) Bochmann, M.; Lancaster, S. J. *J. Organomet. Chem.* **1992**, *434*, C1. (b) S. J. Lancaster, http://www.syntheticpages.org/pages/216.

(0.9 g, 1.6 mmol, 84%). Anal. Calcd for $C_{25}H_{32}HfSi_2$: C, 52.94; H, 5.69. Found: C, 52.69; H, 5.77. ^{1}H NMR (300 MHz, 25 °C, benzene-d_6): δ 7.57−7.52 (m, 2H, C_6-Ind), 7.28−7.15 (m, 4H, C_6-Ind), 6.85−6.81 (m, 3H, C_6-Ind and C_5-Ind), 6.58 (d, J = 3.3 Hz, 1H, C_5-Ind), 5.60 (d, J = 3.3 Hz, 1H, C_5-Ind), 5.53 (d, J = 3.3 Hz, 1H, C_5-Ind), 0.58 (s, 3H, $SiMe_2$), 0.56 (s, 3H, $SiMe_2$), 0.10 (s, 9H, $SiMe_3$), −0.88 (d, ^2J = 11.7 Hz, $HfCH_2$), −1.22 (s, 3H, $HfCH_3$), −2.20 (d, ^2J = 11.7 Hz, $HfCH_2$). ^{13}C NMR (75.47 MHz, 25 °C, benzene-d_6): δ 131.01, 129.47, 126.57, 125.84, 125.67, 125.47, 125.29, 125.4, 125.13, 124.83, 124.61, 124.47 (C_6-Ind), 116.88, 115.59, 112.91, 108.04, 88.34, 84.63 (C_5-Ind), 55.24 (J_{CH} = 105 Hz, $HfCH_2$), 43.84 (J_{CH} = 116 Hz, $HfCH_3$), 3.14 ($SiMe_3$), −1.31 ($SiMe_2$), −2.55 ($SiMe_2$).

(SBI)Zr(CH_2SiMe_3)(μ-Me)$B(C_6F_5)_3$ (7). A 0.24 g (0.5 mmol) sample of (SBI)Zr(Me)CH_2SiMe_3 and 0.26 g (0.5 mmol) of $B(C_6F_5)_3$ were loaded into a 100 mL Schlenk flask. Adding 20 mL of dry toluene gave an orange solution, which was stirred for 10 min. Removal of the solvent under vacuum afforded a yellow crystalline solid, which was washed with 20 mL of light petroleum to yield pure **7** (0.45 g, 90%). Anal. Calcd for $C_{43}H_{32}BF_{15}Si_2Zr$: C, 52.07; H, 3.25. Found: C, 52.11; H, 3.37. ^{1}H NMR (300 MHz, −50 °C, CD_2Cl_2): δ 7.69−6.88 (m, 7H, C_6-Ind and 1H C_5-Ind), 6.30−6.14 (m, 4H, 1H, C_6-Ind and 3H C_5-Ind), 1.07 (s, 3H, $SiMe_2$), 0.88 (s, 3H, $SiMe_2$), 0.13 (d, ^2J = 10.5 Hz, 1H, $ZrCH_2$), −0.08 (s, 9H, $SiMe_3$), −0.69 (br, 3H, μ-Me), −0.97 (d, ^2J = 10.5 Hz, 1H, $ZrCH_2$). ^{13}C NMR (75.47 MHz, −50 °C, CD_2Cl_2): δ 133.20, 130.07, 128.49, 127.99, 127.27, 126.96, 126.59, 125.47, 124.99, 124.38, 123.94, 123.57 (C_6-Ind), 121.93, 115.88, 113.34, 108.55, 91.04, 87.81 (C_5-Ind), 78.07 (J_{CH} = 104 Hz, $ZrCH_2$), −0.78 ($SiMe_3$), −1.18 ($SiMe_2$), −3.95 ($SiMe_2$).

[(SBI)Zr(CH_2SiMe_3)$^+$···$B(C_6F_5)_4^-$] (8). Solid **3** (5 mg, 10 μmol) and $CPh_3[B(C_6F_5)_4]$ (9.3 mg, 10 μmol) were loaded into a 5 mm NMR tube and dissolved in 0.6 mL of toluene-d_8 containing 10 vol % of dry 1,2-difluorobenzene to ensure a homogeneous solution. The conversion to **3** was essentially quantitative. A trace of $SiMe_4$ due to hydrolysis was also observed. There was no change in the NMR spectra of solutions kept in sealed tubes at room temperature over a period of several days. ^{1}H NMR (300 MHz, −20 °C, toluene-d_8/$F_2C_6H_4$, 9:1 v/v): δ 7.5−6.3 (Ind-C_5 and C_6, overlapped with toluene, $F_2C_6H_4$, and byproduct Ph_3CMe), 5.71 (s, 2H, C_5), 5.05 (s, br, 1H, H-3 of C_5), 2.55 (d, 1H, J = 12.3 Hz, $ZrCH_2$), 1.98 (s, 3H, Ph_3CCH_3), 0.77 (s, 3H, $SiMe_2$), 0.54 (s, 3H, $SiMe_2$), −0.27 (d, 1H, J = 12.3 Hz, $ZrCH_2$), −0.64 (s, 9H, $SiMe_3$). ^{13}C NMR (75.5 MHz, 20 °C, tolene-d_8/$F_2C_6H_4$, 9:1 v/v): δ (some of peaks overlapped with solvents and Ph_3CMe) 152.1, 150.6, 147.4, 143.2, 142.2, 138.6, 135.2, 131.9, 130.2, 126.1, 114.5, 85.8 (C_5-Ind), 76.1 ($ZrCH_2$), 52.8 (Ph_3CMe), 30.3 (Ph_3CMe), 1.1 ($SiMe_3$), −3.2 ($SiMe_2$).

(SBI)Hf(CH_2SiMe_3)(μ-Me)$B(C_6F_5)_3$ (9). Complex **6** (0.52 g, 0.91 mmol) and $B(C_6F_5)_3$ (0.55 g, 1.06 mmol) were suspended in cold (−80 °C) toluene (20 mL), and the mixture was slowly warmed to room temperature. The solids dissolved to give a yellow solution from which a fine solid precipitated after stirring for 15 min. The suspension was warmed gently until the precipitate redissolved. Slow cooling of the resulting solution yielded yellow cubic crystals of **9** (0.8 g, 0.74 mmol, 81%). ^{1}H NMR (300 MHz, −50 °C, CD_2Cl_2): δ 7.81−6.9 (m, 7H, C_6-Ind and 1H C_5-Ind), 6.25−6.24 (m, 2H, C_6-Ind and C_5-Ind), 6.00 (m, 1H, C_5-Ind), 5.80 (m, 1H, C_5-Ind), 1.09 (s, 3H, $SiMe_2$), 0.90 (s, 3H, $SiMe_2$), −0.10 (s, 9H, $SiMe_3$), −0.39 (br, 3H, μ-Me), −0.73(d, ^2J = 10.2 Hz, 1H, $HfCH_2$), −1.32 (d, ^2J = 10.2 Hz, 1H, $HfCH_2$). ^{13}C NMR (75.47 MHz, −50 °C, CD_2Cl_2): δ 132.43, 129.39, 129.28, 128.39, 127.57, 125.28 (C_6-Ind), 124.71, 120.70, 113.98, 111.52, 91.62, 87.43 (C_5-Ind), 66.77 (J_{CH} = 102 Hz, $HfCH_2$), 2.9 ($SiMe_3$), −1.15 ($SiMe_2$), −4.0 ($SiMe_2$).

[*rac*-(SBI)Hf$CH_2SiMe_3^+$···$B(C_6F_5)_4^-$] (10). The compound was generated in the NMR tube following the procedure described for **8**. Solutions were thermally stable at room temperature for extended periods of time. The NMR data of a solution of [Hf] = 20 mM are given below. ^{1}H NMR (300 MHz, −10 °C, tolene-d_8/$F_2C_6H_4$, 9:1 v/v): δ 7.2−6.3 (C_6-Ind and C_5-Ind, overlapped with toluene, $F_2C_6H_4$ and byproduct Ph_3CMe), 6.21 (t, 1H, J_{HH} = 7.8 Hz, C_6), 5.54 (s, 1H, C_5), 5.45 (s, 1H, C_5), 4.84 (s, 1H, C_5), 1.98 (s, 3H, Ph_3CMe), 1.90 (d, 1H, J = 12.6 Hz, $HfCH_2$), 0.66 (s, 3H, $SiMe_2$), 0.43 (s, 3H, $SiMe_2$), −0.06 (s, br, 6H, $SiMe_3$), −0.40 (d, 1H, J = 12.7 Hz, $HfCH_2$), −1.75 (s, br, 3H, $SiMe_3$). ^{13}C NMR (tol-d_8 + 10 vol % $F_2C_6H_4$, −10 °C): δ 151.2, 150.7, 147.6, 135.5, 131.1, 130.0, 126.5, 123.4, 121.4, 119.2, 115.3, 113.4, 112.7 (some of peaks were overlapped with solvents and Ph_3CMe), 85.6 (C_5), 83.6 (C_5), 69.1 ($HfCH_2$), 52.8 (Ph_3CMe), 30.7 (Ph_3CMe), −2.5 ($SiMe_3$), −3.8 ($SiMe_2$).

Spectroscopic Characterization of [{(SBI)ZrCH_2SiMe_3}$_2$(μ-Me)][$B(C_6F_5)_4$]. A precooled (−80 °C) dichloromethane-d_2 solution of $[Ph_3C][B(C_6F_5)_4]$ (0.4 mL, 0.1 M, 0.04 mmol) was treated with a dichloromethane-d_2 solution of **3** (0.5 mL, 0.2 M, 0.1 mmol). The sample was mixed cold and immediately transferred to the precooled NMR spectrometer probe (−50 °C). ^{1}H NMR (300 MHz, −50 °C, CD_2Cl_2): major diastereomer: δ 1.05 (s, 3H, $SiMe_2$), 0.90 (s, 3H, $SiMe_2$), 0.02 (s, 18H, $SiMe_3$), −2.03 (d, ^2J = 7.6 Hz, $ZrCH_2$), −2.97 (s, 3H, μ-Me); minor diastereomer: δ 1.03 (s, 3H, $SiMe_2$), 0.90 (s, 3H, $SiMe_2$), −0.01 (s, 18H, $SiMe_3$), −1.77 (d, ^2J = 7.4 Hz, $ZrCH_2$), −2.62 (s, 3H, μ-Me). In both cases the second $ZrCH_2$ resonance is obscured by the $SiMe_3$ signals. Selected ^{13}C NMR (75.47 MHz, −50 °C, CD_2Cl_2): major isomer: δ 84.4 (J_{CH} = 100 Hz, $ZrCH_2$), 10.91 (J_{CH} = 136 Hz, μ-Me).

Spectroscopic Characterization of [{(SBI)Hf(CH_2SiMe_3)}$_2$(μ-Me)][$B(C_6F_5)_4$]. A precooled (−30 °C) solution of $[Ph_3C][B(C_6F_5)_4]$ in bromobenzene-d_5 (0.4 mL, 0.1 M, 0.04 mmol) was treated with a bromobenzene solution of **6** (0.4 mL, 0.2 M, 0.08 mmol). The sample was mixed cold and immediately transferred to a precooled NMR spectrometer probe (−10 °C). ^{1}H NMR (300 MHz, −10 °C, C_6D_5Br): first diastereomer: δ 1.01 (s, 3H, $SiMe_2$), 0.85 (s, 3H, $SiMe_2$), 0.21 (s, 18H, $SiMe_3$), −0.51 (d, ^2J = 9 Hz, $HfCH_2$), −1.93 (d, ^2J = 9 Hz, $HfCH_2$), −2.47 (s, 3H, μ-Me); second diastereomer: δ 1.01 (s, 3H, $SiMe_2$), 0.85 (s, 3H, $SiMe_2$), 0.18 (s, 18H, $SiMe_3$), −0.60 (d, ^2J = 8.9 Hz, $HfCH_2$), −2.13 (d, ^2J = 8.9 Hz, $HfCH_2$), −2.69 (s, 3H, μ-Me).

PGSE and HOESY Measurements. All the PGSE NMR measurements were performed on a Bruker Avance DRX 400 spectrometer equipped with a direct QNP probe and a z-gradient coil controlled by a Great 1/10 gradient unit, by using the standard stimulated echo pulse sequence[42] at 295 K without spinning. The shape of the gradients was rectangular, their duration (δ) was 4 ms, and their strength (G) was varied during the experiments. All the spectra were acquired using 32K points, 16 or 64 scans depending on concentration, and a spectral width of 5000 Hz and were processed with a line broadening of 3.0 Hz. The experiments were carried out with a total recycle time of ca. 10 s. The semilogarithmic plots of $\ln(I/I_0)$ vs G^2 were fitted using a standard linear regression algorithm obtaining an R factor always better than 0.99. Gradients were calibrated using the diffusion of HDO in D_2O;[43] data at different temperatures were estimated by interpolation of the data reported by Mills, giving $D_{HDO} = 1.748 \times 10^{-9}$ m^2 s^{-1}, at 295 K. Data analysis was carried out according to a literature procedure[44] using the residual toluene resonance at 2.09 ppm as internal standard. Viscosity of C_7D_8 was estimated to be 0.616 cP at 295 °C by interpolation of the data reported for C_7H_8[45] applying the correction $\eta(C_7D_8) = 1.07 \times \eta(C_7H_8)$.[46]

(42) Valentini, M.; Rüegger, H.; Pregosin, P. S. *Helv. Chim. Acta* **2001**, *84*, 2833, and references therein.
(43) Mills, R. *J. Phys. Chem.* **1973**, *77*, 685.
(44) Zuccaccia, D.; Sabatini, S.; Bellachioma, G.; Cardaci, G.; Clot, E.; Macchioni, A. *Inorg. Chem.* **2003**, *42*, 5465.
(45) *CRC Handbook of Chemistry and Physics*, 67th ed.; Weast, R. C., Ed.; Chemical Rubber: Cleveland, 1986.

van der Waals volumes (Å^3) used for calculation were as follows: toluene-d_8, 86.6; (SBI)Zr(CH_2SiMe_3)(μ-Me)B(C_6F_5)$_3$, 625; [(SBI)Zr(CH_2SiMe_3)]$^+$[B(C_6F_5)$_4$]$^-$, 690.

Semiquantitative two-dimensional ^{19}F,^{1}H HOESY NMR experiments were acquired using the standard four-pulse sequence, a recycle delay of 1s, and a mixing time of 200−500 ms. A total of 512 increments were acquired using 32−256 scans per increment depending on concentration and digitalized in 1024 data points.

Crystal Structure Analyses. Crystals coated in dried perfluoropolyether oil were mounted on glass fibers and fixed in a cold nitrogen stream. Diffraction intensities of **3** were measured on a Rigaku R-Axis IIc image-plate diffractometer equipped with a rotating anode X-ray source; those of **6** and **9** were measured on a Nonius KappaCCD diffractometer. Mo Kα radiation and graphite monochromators were used. Data were processed using the DENZO/SCALEPACK programs.[47] The structure was determined by the direct methods routines in the XS[48] or SHELXS[49] programs and refined by full-matrix least-squares methods, on F^2's, in XL or SHELXL. Non-hydrogen atoms were refined with anisotropic displacement parameters. In **3**, H(21x) and H(21y) were refined freely and isotropically; all other hydrogen atoms were included in idealized positions and their U_{iso} values were set to ride on the U_{eq} values of the parent carbon atoms. In the final difference maps, the highest peak (ca. 0.5 e Å^{-3}) was close to C(21). In **6**, the hydrogen atoms of the methyl group C(30) were allowed to rotate. The hydrogen atoms H(21x) and H(21y) were refined freely. In the final difference map, the highest peaks (to ca. 0.77 e Å^{-3}) were close to the hafnium atom. In **9**, attempts to refine the H atoms on C(30) and C(21) freely failed and the refinement became unstable. The methyl group around C(40) was allowed to rotate to determine the best position of the hydrogen atoms. No hydrogen atoms at all were fixed in the disordered toluene molecule. In the final difference map, the highest peaks (to ca. 1.41 e Å^{-3}) were close to the silicon atom Si(2).

Scattering factors for neutral atoms were taken from the literature.[50] Computer programs were run on a Silicon Graphics Indy at the University of East Anglia or on a DEC-AlphaStation 200 4/100 in the Biological Chemistry Department, John Innes Centre.

Acknowledgment. This work was supported by the Engineering and Physical Sciences Research Council, the European Commission (Contract Nr. HPRN-CT2000-00004) and the Ministero dell'Istruzione, dell'Università e della Ricerca (MIUR, Rome, Italy), Programma di Rilevante Interesse Nazionale, Cofinanziamento 2002−2003.

Supporting Information Available: Details of HOESY spectra of **7** and **8** and tables of X-ray diffraction data for **3**, **6**, and **9**. This material is available free of charge via the Internet at http://pubs.acs.org.

OM049248D

(46) Morresi, A.; Paolantoni, M.; Sassi, P.; Aluigi, A. *J. Mol. Phys.* **2002**, *100*, 3677.

(47) Otwinowski, Z.; Minor, W. *Methods in Enzymology, Macromolecular Crystallography, Part A*; Carter, C. W., Sweet, R. M., Eds.; Academic Press: New York, 1997; Vol. 276, pp 307−326.

(48) Sheldrick, G. M. *SHELXTL* package, including XS for structure determination, XL for refinement, and XP for molecular graphics; Siemens Analytical Inc., 1995.

(49) Sheldrick, G. M. *SHELX-97*, Programs for crystal structure determination (SHELXS) and refinement (SHELXL); University of Göttingen: Germany, 1997.

(50) *International Tables for X-ray Crystallography*; Kluwer Academic Publishers: Dordrecht, 1992; Vol. C, pp 500, 219, and 193.